Fig. 5

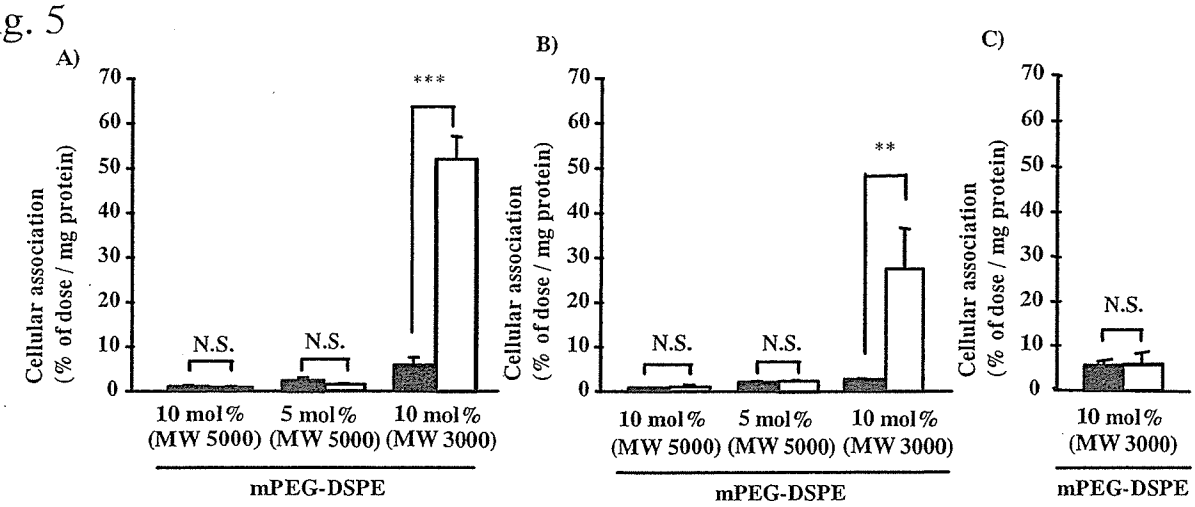

Fig. 6

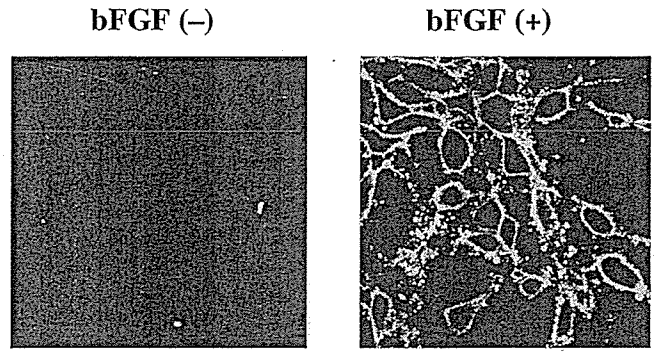

Fig. 7

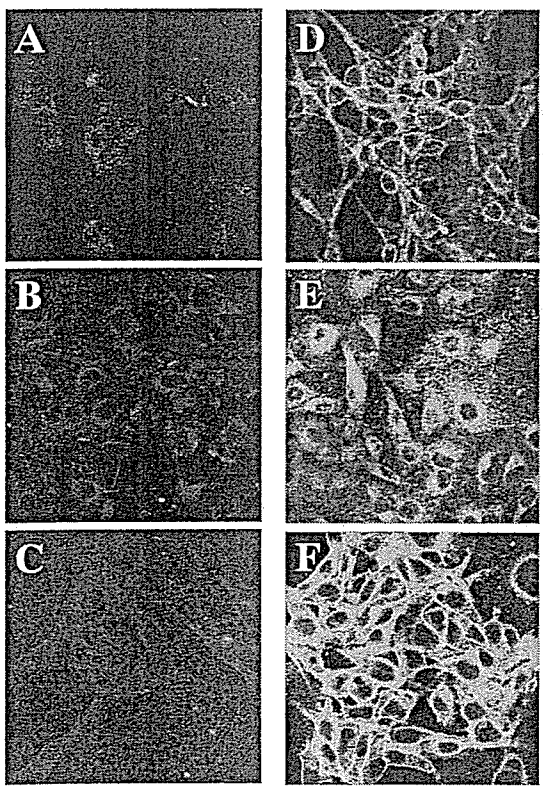

Fig. 8

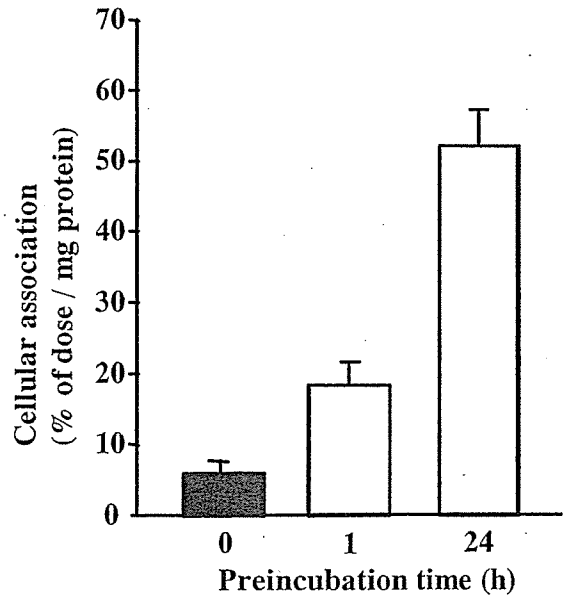

Available online at www.sciencedirect.com
ScienceDirect
Biomaterials 28 (2007) 532–539
Biomaterials
www.elsevier.com/locate/biomaterials

The potential role of fucosylated cationic liposome/NFκB decoy complexes in the treatment of cytokine-related liver disease

Yuriko Higuchi, Shigeru Kawakami, Fumiyoshi Yamashita, Mitsuru Hashida*

Department of Drug Delivery Research, Graduate School of Pharmaceutical Sciences, Kyoto University, Kyoto 606-8501, Japan

Received 15 June 2006; accepted 25 August 2006
Available online 18 September 2006

Abstract

Cytokine production by Kupffer cells, which is regulated by NFκB, causes severe liver injury in endotoxin syndrome. NFκB decoy has been reported to inhibit NFκB-mediated transcription. The purpose of this study is to inhibit LPS-induced cytokine production by Kupffer cell-targeted delivery of NFκB decoy using fucosylated cationic liposomes (Fuc-liposomes). Cholesten-5-yloxy-*N*-{4-[(1-imino-2-L-thiofucosyl-ethyl)-amino] butyl-}formamide (Fuc-C4-Chol) was synthesized to prepare Fuc-liposomes. Tissue accumulation, intrahepatic distribution and serum cytokine concentrations were investigated after intravenous injection of Fuc-liposomes/NFκB decoy complexes. Intravenously injected Fuc-liposome complexes rapidly and highly accumulated in the liver while little naked NFκB decoy accumulated in the liver. An intrahepatic distribution study showed that Fuc-liposome complexes are mainly taken up by non-parenchymal cells. The liver accumulation of Fuc-liposome complexes was inhibited by $GdCl_3$ pretreatment, which selectively inhibited Kupffer cell uptake. This result suggested that Kupffer cells contribute to liver accumulation. TNFα, IFNγ, ALT and AST serum levels in LPS-infected mice were significantly attenuated by treatment with Fuc-liposome complexes compared with naked NFκB decoy. Fuc-liposome complexes also reduced the amount of activated NFκB in the liver nuclei. Fuc-liposomes would be a useful carrier for Kupffer cell-selective delivery of NFκB decoy by intravenous injection.

Keywords: Fucosylated cationic liposome; Gene delivery; Gene therapy; Targeting; NFκB decoy; Kupffer cell

1. Introduction

Several forms of hepatic failure, including endotoxin syndrome, are associated with inflammatory cytokines produced by Kupffer cells [1,2]. Since NFκB regulates inflammatory cytokine production [3,4] the inhibition of NFκB activation in Kupffer cells would offer a new treatment for liver failures. Recently, Wrighton et al. [5] and Foxwell et al. [6] reported that the adenoviral gene transfer of super-repressor IκB effectively suppressed NFκB, however the inflammatory reaction and high immunogenicity of the adenoviral vector itself presented a serious obstacle. On the other hand, it was demonstrated recently that NFκB decoy inhibited the production of cytokines, such as TNFα, IL-1β, IFNγ and IL-12 [7–9]. Therefore, NFκB decoy would be an attractive option for the treatment of cytokine-related liver diseases without any marked immunogenic effects [10].

To establish NFκB decoy therapy, it is necessary to develop a Kupffer cell-targeting carrier for NFκB decoy because of the low uptake of naked NFκB decoy by cells [11]. In general, the receptor-mediated endocytosis system is potentially useful for cell-specific delivery, including carbohydrate receptors expressed on liver cells [12]. As far as gene delivery is concerned, we have shown that mannosylated cationic liposomes can deliver pDNA to NPC [13–15] including Kupffer cells and sinusoidal endothelial cells through the recognition of mannose receptors highly expressed on NPC.

Regarding Kupffer cell-selective delivery, we have demonstrated that fucosylated protein is preferentially taken up by Kupffer cells [16] through fucose receptor recognition, which is uniquely exhibited by Kupffer cells [17]. Taking this into consideration, we have synthesized a

*Corresponding author. Tel.: +81 75 753 4545; fax: +81 75 753 4575.
E-mail address: hashidam@pharm.kyoto-u.ac.jp (M. Hashida).

0142-9612/$ - see front matter © 2006 Elsevier Ltd. All rights reserved.
doi:10.1016/j.biomaterials.2006.08.045

novel fucosylated lipid, cholesten-5-yloxy-*N*-{4-[(1-imino-2-L-thiofucosyl-ethyl)-amino] butyl}formamide (Fuc-C4-Chol), which poses fucose as a ligand for receptor recognition, a cholesterol derivative for stable insertion into liposomes and carrying a positive charge [18]. Therefore, fucosylated cationic liposomes (Fuc-liposomes) with a high density of fucose and a positive charge on the surface of liposomes containing more Fuc-C4-Chol, could achieve better Kupffer cell-selective delivery of NFκB decoy. Moreover, considering that the site of action of NFκB decoy is the cytoplasm, we chose dioleoylphosphatidylethanolamine (DOPE), which helps the gene to escape from endosomes through a conformational change at low pH [19].

The purpose of this work was to develop Kupffer selective targeting of NFκB decoy to Kupffer cells after intravenous injection. We prepared Fuc-liposome using Fuc-C4-Chol and investigated the distribution of Fuc-liposomes/NFκB decoy complexes after intravenous injection. The inhibitory effect of cytokine production by Fuc-liposomes/NFκB complexes was also examined. This is an initial report of the Kupffer cell-selective delivery of NFκB decoy and its therapeutic effect using Fuc-liposomes given by intravenous injection.

2. Material and methods

2.1. Materials

N-(4-aminoethyl) carbamic acid tert-butyl erter was purchased from Tokyo Kasei Kogyo Co. Ltd. (Tokyo, Japan). DOPE was purchased from Avanti Polar Lipids Inc. (Alabaster, AL, USA). Cholesteryl chloroformate, heparin and collagenase and D-(+)-galactosamine were purchased from Sigma Chemicals Pvt. Ltd. (St Louis, MO, USA). Oligonucleotides (NFκB decoy: 5′-AGTTGAGGGGACTTTCCCAGGC-3′, 5′-GCCT GGGAAAGTCCCCTCAACT-3′, random decoy: 5′-TTGCCGTACCT GACTTAGCC-3′, 5′-GGCTAAGTCAGGTACGGCAA-3′) were purchased from Operon Biotechnologies Inc. (Tokyo, Japan). L-(−)-Fucose, ethylene glycol-*bis* (*b*-aminoethylether)-*N*,*N*,*N*′,*N*′-tetraacetic acid (EGTA), Clear-Sol I and cholesterol were purchased from Nacalai Tesque Inc. (Kyoto, Japan). MEGALABEL™ 5′-End Labeling Kit was purchased from Takara Bio Inc. (Shiga, Japan). Soluene-350 was purchased from Perkin Elmer Inc. (Boston, MA, USA). An NAP-5 column was purchased from Amersham Biosciences Co. (Piscatway, NJ, USA). Trypan blue was purchased from Invitrogen Co. (Grand Island, NY, USA). Mouse TNFα BD OptEIA™ ELISA Kit was purchased from Becton, Dickinson and Company (Mississauga, Canada). FractionPREP™ Nuclear/Cytosol Fraction Kit was purchased from BioVision Inc. (Mountain View, CA, USA). Chemiluminescent NFκB Activation Assay Kit was purchased from Oxford Biomedical Research Inc. (Oxford, MI, USA). D-(+)-mannose and transaminase CII test Wako were purchased from Wako Pure Chemical Industries Ltd. (Osaka, Japan).

2.2. Animals

Female ICR mice (5-week old, 22–24 g) and female C57BL/6 mice (6-week old, 18–20 g) were obtained from Shizuoka Agricultural Cooperative Association for Laboratory Animals (Shizuoka, Japan). All animal experiments were carried out in accordance with the Principles of Laboratory Animal Care as adopted and promulgated by the US National Institutes of Health and with the Guidelines for Animal Experiments of Kyoto University.

2.3. Radiophosphorylation of decoy oligonucleotides

Annealed NFκB decoy was labeled with [γ-^{32}P] ATP using MEGALABEL™ 5′-End Labeling Kit with some modification as reported previously [11]. Briefly, oligonucleotides, [γ-^{32}P] ATP and T4 polynucleotide kinase were mixed in phosphorylation buffer. After a 30-min incubation at 37 °C, the mixture was incubated for 10 min at 70 °C in order to inactivate T4 polynucleotide kinase. Then, the mixture was purified by gel chromatography using a NAP 5 column and eluted with 10 mM Tris–Cl and 1 mM EDTA (pH 8.0). The fractions containing the derivatives were selected based on their radioactivity.

2.4. Synthesis of Fuc-C4-Chol

Fuc-C4-Chol was synthesized as reported previously [18,20]. Briefly, cholesteryl chloroformate and *N*-(4-aminobutyl)carbamic acid *tert*-butyl ester were reacted in chloroform for 24 h at room temperature. A solution of trifluoroacetic acid and chloroform was added dropwise and the mixture was stirred for 4 h at 4 °C. The solvent was evaporated to obtain *N*-(4-aminobutyl)-(cholesten-5-yloxyl)formamide which was then combined with 2-imino-2-methoxyethyl-1-thiofucoside and the mixture was stirred for 24 h at room temperature. After evaporation, the resultant material was suspended in water, dialyzed against distilled water for 48 h (12 kDa cut-off dialysis tubing), and then lyophilized. Man-C4-Chol and Gal-C4-Chol were synthesized in the similar manner using mannose or galactose.

2.5. Preparation of liposomes and their complex with NFκB decoy

Fuc-C4-Chol was mixed with DOPE in chloroform at a molar ratio of 3:2 and the mixture was dried, vacuum desiccated and resuspended in sterile 5% dextrose. After hydration for 30 min at room temperature, the dispersion was sonicated for 10 min in a bath sonicator and then for 3 min in a tip sonicator to form liposomes. The particle size of the liposomes and liposomes/NFκB decoy complexes were measured using dynamic light scattering spectrophotometer (LS-900, Otsuka Electronics, Osaka, Japan). The zeta potential of liposomes and liposome/NFκB decoy complexes were measured by Nano ZS (Malvern Instruments Ltd., Malvern, WR, UK). The preparation of liposomes/NFκB decoy complexes for in vivo use was carried out by the method of Kawakami et al. [13]. Equal volumes of NFκB decoy and stock liposome solution were diluted with 5% dextrose at room temperature. Then, the NFκB decoy solution was added rapidly to the liposome solution and the mixture was agitated rapidly by pumping it up and down twice in the pipet tip. The mixture was then left at room temperature for 30 min. The theoretical charge ratio of lipid/NFκB decoy was calculated as a molar ratio of Fuc-C4-Chol (monovalent) to a nucleotide unit (average molecular weight 330) [21]. Man-liposomes and Gal-liposomes were prepared in the similar manner.

2.6. In vivo distribution

The in vivo distribution was examined as previously reported [22]. Fuc-liposomes/NFκB decoy complexes in 300 μl 5% dextrose solution were intravenously injected into mice. Blood was collected from the vena cava at 1, 3, 10, 30 and 60 min, and mice were killed at each collection time point. Liver, kidney, spleen, heart and lung were removed, washed with saline, blotted dry and weighed. Immediately prior to blood collection, urine was also collected directly from the urinary bladder. Ten μl blood and 200 μl urine, and a small amount of each tissue were digested with Soluene-350 (0.7 ml for blood, urine and tissues) by incubation overnight at 54 °C. Following digestion, 0.2 ml isopropanol, 0.2 ml 30% hydroxyperoxide, 0.1 ml 5 M HCl, and 5.0 ml Clear-Sol I were added. The samples were stored overnight, and radioactivity was measured in a scintillation counter (LSA-500, Beckman, Tokyo, Japan).

2.7. Intrahepatic distribution

The intrahepatic distribution of Fuc-liposomes/[^{32}P] NFκB decoy complexes was determined as in our previous report [18]. Five minutes after intravenous injection of NFκB decoy or Fuc-liposomes/[^{32}P] NFκB decoy complexes, each mouse was anesthetized with diethyl ether and the liver was perfused with pre-perfusion buffer (Ca^{2+}, Mg^{2+}-free Hanks buffer, pH 7.4 containing 1000 units/L heparin and 0.19 g/L EGTA) for 6 min at 5 ml/min followed by Hanks buffer containing 5 mM $CaCl_2$ and 220 units/ml collagenase (Type I) (pH 7.4) for 6 min at 5 ml/min. After discontinuation of the perfusion, the liver was removed and the liver cells were dispersed in ice-cold Hanks-HEPES buffer. The cell suspension was filtered through cotton gauze, followed by centrifugation at 50*g* for 1 min at 4 °C. The pellet containing parenchymal cells (PC) was washed four times with ice-cold Hanks-HEPES buffer. The supernatant containing NPC was collected and purified by centrifugation at 50*g* for 1 min at 4 °C (four times). PC and NPC suspensions were centrifuged at 340*g* for 10 min. PC and NPC were then resuspended separately in ice-cold Hanks-HEPES buffer (final volume 2 ml). The cell number and viability were determined by the trypan blue exclusion method. The radioactivity of 500 μl of each cell suspension was measured by the same method as for the in vivo distribution. To investigate the contribution of Kupffer cells on liver accumulation of Fuc-liposome/NFκB decoy complex, mice were pretreated with $GdCl_3$ (30 mg/kg) 24 h before experiment.

2.8. Animal treatment protocol

For cytokine secretion assessment, blood was collected from ICR mice 1 h for TNFα, 6 h for IFNγ after intravenous injection of LPS (0.4 mg/kg). The blood was allowed to coagulate for 2–3 h at 4 °C and serum was isolated as the supernatant fraction following centrifugation at 2000*g* for 20 min. The serum samples were immediately stored at −80 °C. The amounts of TNFα and IFNγ were analyzed using an OptiEIA™ ELISA Kit according to the manufacturer's protocol. For severe liver injury model, C57BL/6 mice were injected intraperitoneally with LPS (0.05 mg/kg) and D-galactosamine (1000 mg/kg) in pyrogen-free saline. The blood was collected from mice 3 h after LPS and D-galactosamine treatment. The blood was allowed to coagulate for 2–3 h at 4 °C and serum was isolated as the supernatant fraction following centrifugation at 2000*g* for 20 min. Serum ALT and AST were measured with transaminase C II test Wako according to the manufacturer's protocol.

2.9. Enzyme immunoassay (EIA) for nuclear NFκB measurement

Liver was removed, washed with ice-cold saline and blotted dry. A small amount of liver was homogenized in phosphate-buffered saline. Pellets of cells were obtained by centrifugation at 500*g* for 2 min, and a nuclear extract was prepared using a Nuclear/Cytosol Fraction Kit. The amounts of NFκB in the nuclei were measured with an NFκB Activation Assay Kit according to the manufacturer's protocol.

2.10. Statistical analyses

Statistical comparisons were performed by Student's *t*-test for two groups and one-way ANOVA for multiple groups. Post hoc multiple comparisons were made by using Tukey's test.

3. Results

3.1. Particle size and zeta potential of Fuc-liposomes and their complex with NFκB decoy

The mean diameter and zeta potential of Fuc-liposomes or Fuc-liposomes/NFκB decoy complexes in 5% dextrose were mesured. The mean diameter of the Fuc-liposomes and Fuc-liposomes/NFκB decoy complexes were 79.5 ± 1.45 nm ($n = 3$) and 64.5 ± 1.84 nm ($n = 3$), respectively. After forming complexes with NFκB decoy, the charge on the surface of the Fuc-liposomes/NFκB decoy complexes was reduced to 37.4 ± 2.84 nm ($n = 3$) compared with Fuc-liposomes (62.0 ± 0.91 nm, $n = 3$) but still slightly cationic.

3.2. Rapid and high liver accumulation of Fuc-liposome/NFκB decoy complexes

Fig. 1 shows the time-courses of the radioactivity in blood, spleen, liver and kidney after intravenous injection of naked [^{32}P] NFκB decoy or Fuc-liposomes/[^{32}P] NFκB decoy complex. High and rapid liver accumulation of the Fuc-liposome/[^{32}P] NFκB decoy complex was observed. Following liver accumulation, the Fuc-liposome/[^{32}P]

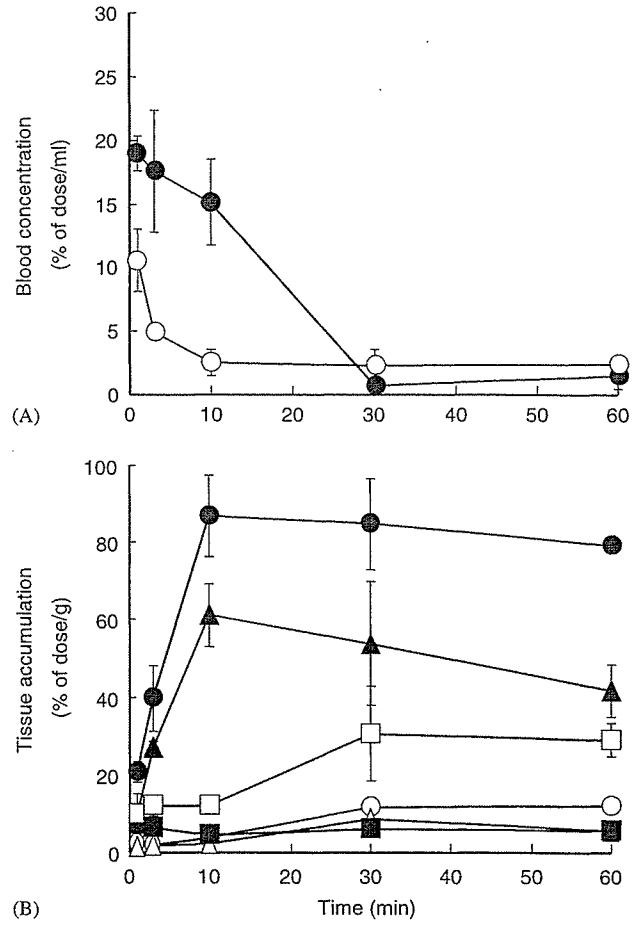

Fig. 1. Blood concentration of [^{32}P] naked NFκB decoy (○) and Fuc-liposome/[^{32}P] NFκB decoy complex (●) (A) and tissue accumulation of [^{32}P] naked NFκB decoy (liver ○, spleen △, kidney □) and Fuc-liposome/[^{32}P] NFκB decoy complex (liver ●, spleen ▲, kidney ■) after intravenous injection into mice (B). [^{32}P] NFκB decoy (NFκB decoy 20 μg/mouse) was complexed with Fuc-liposomes at a charge ratio of 1.0:2.3 (−:+). Radioactivity was determined in blood, liver, lung and spleen after 1, 3, 10, 30 and 60 min.

NFκB decoy complex highly accumulated in the spleen, while the naked NFκB decoy did not highly accumulate in the liver or spleen. The highest accumulation of naked [^{32}P] NFκB decoy was observed in the kidney. Although naked [^{32}P] NFκB decoy rapidly disappeared from the blood circulation, the Fuc-liposome/[^{32}P] NFκB decoy complex maintained a higher blood concentration than the naked [^{32}P] NFκB decoy.

3.3. NPC accumulation of Fuc-liposome/NFκB decoy complex

After intravenous injection of Fuc-liposome/[^{32}P] NFκB decoy complex, the radioactivity in the liver was preferentially recovered from the NPC fraction with the radioactivity ratio of NPC to PC (NPC/PC ratio on a cell-number basis) in the liver being approximately 4.49 (Fig. 2). In contrast, naked [^{32}P] NFκB decoy had an NPC/PC ratio of 0.66 (Fig. 2). The total liver accumulation of Fuc-liposome/[^{32}P] NFκB decoy complex was higher than that of the naked [^{32}P] NFκB decoy.

3.4. Inhibition of Fuc-liposome/NFκB decoy complex liver accumulation by $GdCl_3$ pretreatment

$GdCl_3$ pretreatment inhibits the uptake of Kupffer cells after intravenous injection [23,24]. The hepatic uptake of Fuc-liposome/[^{32}P] NFκB complex was effectively inhibited by $GdCl_3$ pretreatment (Fig. 3). On the other hand, the uptake by spleen and lung was slightly increased by $GdCl_3$ pretreatment.

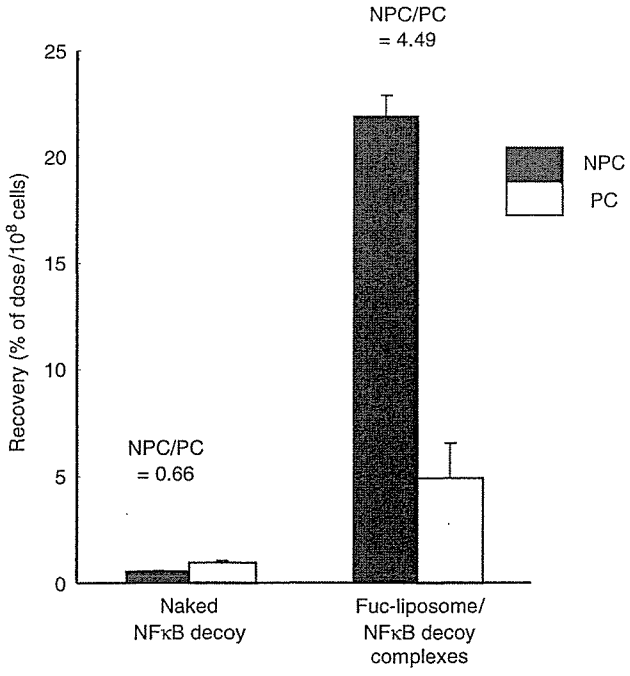

Fig. 2. Intrahepatic distribution of [^{32}P] naked NFκB decoy (A) and Fuc-liposome/[^{32}P] NFκB decoy complex (B) (NFκB decoy 20 μg/mouse) after intravenous injection into mice. [^{32}P] NFκB was complexed with Fuc-liposomes at a charge ratio of 1.0:2.3 (−:+). Radioactivity was determined in NPC (■) and PC (□). Each value represents the mean ± S.D. ($n = 4$).

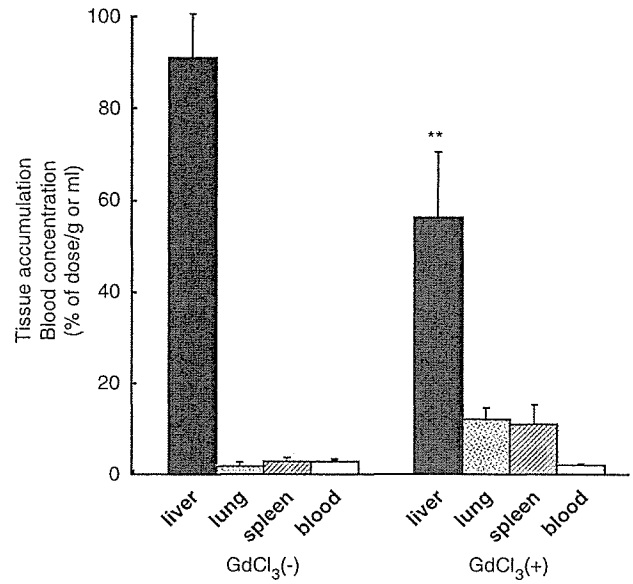

Fig. 3. Tissue accumulation of Fuc-liposome/[^{32}P] NFκB decoy complex (NFκB decoy 20 μg/mouse) after intravenous injection into mice, with or without $GdCl_3$ pretreatment. [^{32}P] NFκB decoy was complexed with Fuc-liposomes at a charge ratio of 1.0:2.3 (−:+). Radioactivity was determined in blood, liver, lung and spleen after 5 min. Each value represents the mean ± S.D. ($n = 3$). Significant difference $^{**}P < 0.01$.

3.5. Suppression of inflammatory cytokine production by Fuc-liposome/NFκB decoy complexes

To confirm that NFκB complexed with Fuc-liposomes effectively suppressed the production of inflammatory cytokines by Kupffer cells in vivo, the serum concentration of TNFα was measured using ELISA (Fig. 4). Control mice were treated with 5% dextrose after injection of LPS. The serum level of TNFα increased dramatically after LPS treatment as expected, and in vivo Kupffer cell-targeted delivery of NFκB decoy by Fuc-liposomes blocked the increase in the production of TNFα (Fig. 4). On the other hand, intravenously injected naked NFκB decoy and Fuc-liposome/random decoy complexes did not affect the serum level of TNFα (Fig. 4). The same amount of NFκB decoy complexed with Man-liposomes slightly reduced the serum level of TNFα (Fig. 4). After LPS treatment, the serum level of IFNγ (2.57 ± 0.82 ng/ml, $n = 4$), which is also regulated by NFκB, was also significantly reduced by Fuc-liposome complexes (0.246 ± 0.122 ng/ml, $n = 4$) but not by naked NFκB decoy (2.57 ± 1.30 ng/ml, $n = 4$).

3.6. Suppression of liver enzyme production by Fuc-liposome/NFκB decoy complexes

To confirm that NFκB complexed with Fuc-liposomes effectively suppressed liver injury, the serum concentrations

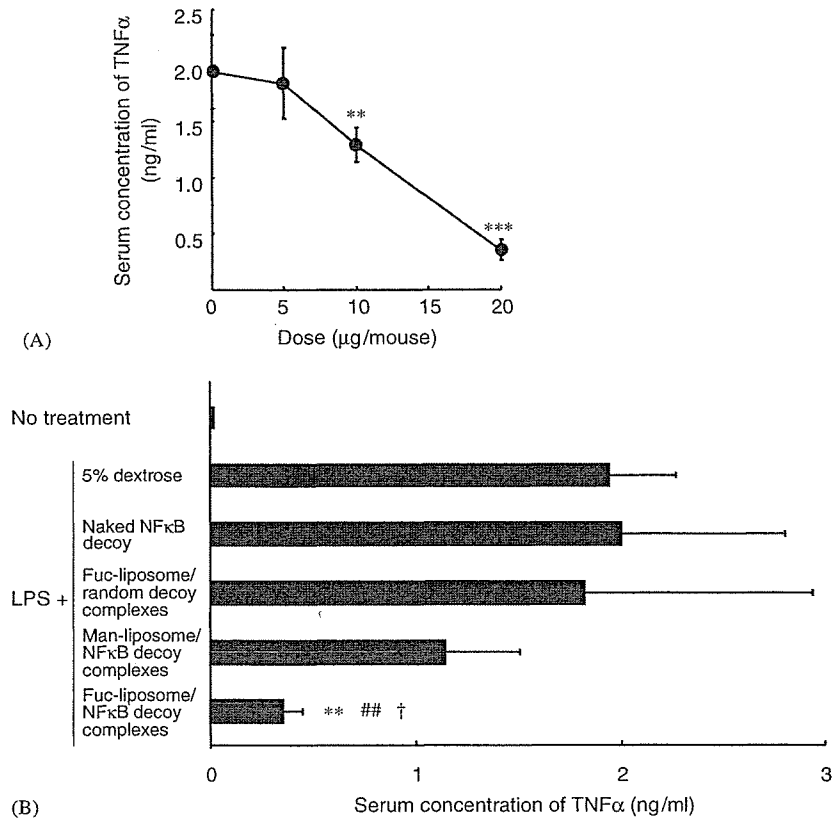

Fig. 4. Inhibitory effect of Fuc-liposome/NFκB decoy complex on the production of TNFα at different doses (A) and comparison with naked NFκB decoy and Fuc-liposome/NFκB decoy complexes (NFκB decoy or random decoy 20 μg/mouse) (B). Serum concentration of TNFα was determined by ELISA. One minute after intravenous administration of LPS, Fuc-liposome/NFκB decoy complexes were intravenously injected into mice. Blood was collected from the vena cava at 1 h. Each value represents the mean ± S.D. ($n = 3-4$). Significant difference $^{***}P<0.001$; $^{**}P<0.01$ v.s. dose of 0 μg of NFκB decoy/mouse in (A), $^{**}P<0.01$ v.s. LPS; $^{\#\#}P<0.01$ v.s. LPS + naked NFκB decoy; $^{\dagger}P<0.05$ v.s. Man-liposome/NFκB decoy complexes in (B).

of ALT and AST were assessed (Fig. 5). Control mice were treated with 5% dextrose after injection of LPS and D-galactosamine. The serum levels of ALT and AST increased dramatically after LPS with D-galactosamine treatment as expected, and in vivo Kupffer cell targeted delivery of NFκB decoy by Fuc-liposomes blocked the increase in the production of ALT and AST (Fig. 5). On the other hand, intravenously injected naked NFκB decoy had no effect on the serum levels of ALT and AST (Fig. 5). Fuc-liposome/random decoy complex also did not reduce the serum level of ALT and AST (data not shown).

3.7. Prevention of NFκB activation by Fuc-liposome/NFκB decoy complexes

In response to inflammatory stimuli, IκB protein degraded and allowed NFκB to translocate into the nucleus to initiate gene expression of inflammatory cytokines. The amount of activated NFκB in the nuclei was measured by EIA to confirm the inhibitory effect of Fuc-liposome complexes on the activation of NFκB. After LPS treatment, the amount of activated NFκB was dramatically increased. However, after injection of Fuc-liposome complexes, the amount of activated NFκB in nuclei did not increase following LPS treatment (Fig. 6).

4. Discussion

Recently, new techniques to inhibit target gene expression using oligonucleotides, such as decoy oligonucleotides, antisense DNA, ribozyme and siRNA, have been developed, and these are expected to be attractive treatments without side effects on genome DNA compared with pDNA. However, oligonucleotides are easily degraded in blood and rapidly metabolized and, therefore, potential carriers have to be developed capable of carrying enough oligonucleotide to produce a therapeutic effect. As far as liver failure is concerned, Kupffer cells, hepatic resident macrophages, play an important role in producing several kinds of systemic cytokines [25,26]. Furthermore, because intravenous injection is a non-invasive method that does not require special techniques, intravenous injectable carrier is desirable in clinical situations. Therefore, the purpose of this study is to develop a Kupffer cell-selective delivery system for NFκB decoy by intravenous injection and to suppress cytokine production.

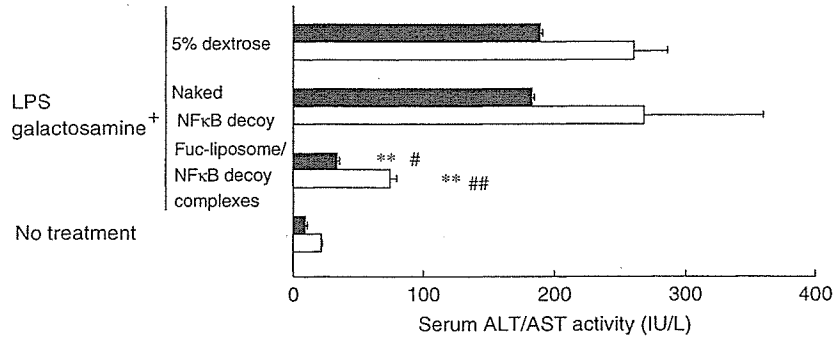

Fig. 5. Inhibitory effect of Fuc-liposome/NFκB decoy complex on liver enzyme injury. One min after intravenous administration of LPS with D-Galactoasmine, Fuc-liposome/NFκB decoy complex or naked NFκB decoy (NFκB decoy 20 μg/mouse) was intravenously injected into mice. Blood was collected from the vena cava at 3 h. Each value represents the mean ± S.D. ($n = 4$). Significant difference $^{**}P<0.01$ v.s. + 5% dextrose; $^{\#}P<0.05$; $^{\#\#}P<0.01$ v.s. + naked NFκB decoy.

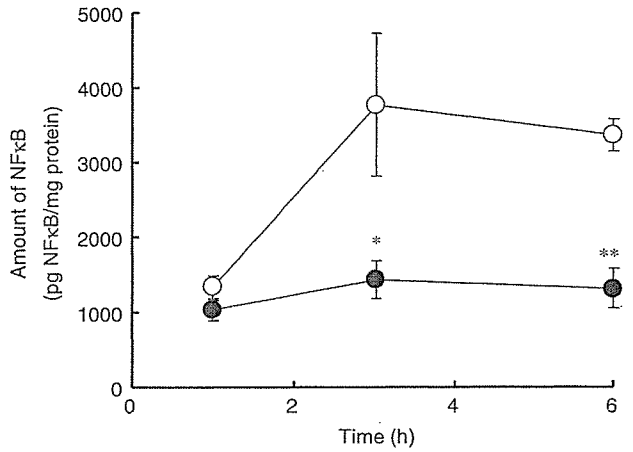

Fig. 6. Inhibitory effect of Fuc-liposome/NFκB decoy complex on NFκB activation in the nuclei. One min after intravenous administration of LPS, Fuc-liposome/NFκB decoy complex (20 μg/mouse) was intravenously injected into mice (●). Control mice were treated with 5% dextrose after injection of LPS (○). Liver was excised from mice at 1, 3 and 6 h. Each value represents the mean ± S.D. ($n = 3-4$). Significant difference $^{**}P<0.01$; $^{*}P<0.05$.

In order to investigate Kupffer cell-selective delivery of NFκB decoy using Fuc-liposomes, the tissue accumulation and intrahepatic distribution of Fuc-liposome/[^{32}P] NFκB decoy complexes was examined after intravenous injection (Fig. 1). Rapid and high liver accumulation of Fuc-liposome/[^{32}P] NFκB decoy complexes was observed. Moreover, Fuc-liposome/NFκB decoy complexes were preferentially taken up by NPC (Fig. 2). To confirm the contribution of Kupffer cells to NPC accumulation, the hepatic uptake of Fuc-liposome/NFκB decoy complex was compared with and without $GdCl_3$ pretreatment, because $GdCl_3$ pretreatment, which inhibits the uptake ability of Kupffer cells without any inflammation by other liver cells, was widely used to analyze Kupffer cell function including uptake and cytokines production etc. [23,24]. The liver accumulation was lower with $GdCl_3$ pretreatment than without it (Fig. 3), which strongly supported Fuc-liposome/NFκB decoy complexes being efficiently taken up by Kupffer cells. This uptake characteristic agrees with the results of the uptake of Fuc-BSA [17]. It has been reported that after single injection of $GdCl_3$ Kupffer cells but not spleen macrophage strongly inhibited receptor mediated binding [23]. This may explain the fact that the spleen uptake of NFκB decoy/Fuc-liposome complexes was increased under $GdCl_3$ treatment (Fig. 3).

After intravenous injection, the distribution of a macromolecule is basically decided by its physicochemical properties, including size and charge. The kidney and liver play an important role in the disposition of macromolecules circulating in the blood [27]. Macromolecules with a molecular weight of less than 50,000 (approximately 6 nm in diameter) are susceptible to glomerular filtration and are excreted into the urine [28]. As far as the distribution of NFκB decoy is concerned, although [^{32}P] NFκB decoy rapidly disappeared from the blood, the Fuc-liposome/NFκB decoy complexes circulated for a little longer (Fig. 1). Considering that the molecular weight of NFκB decoy is about 13,000, this result indicates that Fuc-liposome/NFκB decoy complexes escape rapid glomerular filtration and increase the stability of NFκB decoy in the blood.

It is well known that NFκB decoy can be bound by activated NFκB and inhibits the transfer activated NFκB to the nuclei, consequently inhibiting the transcription of NFκB [29]. To determine the inhibitory mechanism of cytokine production by Fuc-liposome/NFκB decoy complexes, the amount of NFκB in the nuclei was measured by EIA. After injection of Fuc-liposome/NFκB decoy complexes, the amount of NFκB in the nuclei was lower than that after only LPS treatment (Fig. 4). This result shows that NFκB decoy delivered by Fuc-liposomes can inhibit the transfer of activated NFκB to nuclei. Moreover, Fuc-liposome/NFκB decoy complexes can inhibit the production of TNFα and IFNγ (Fig. 4), the expression of which is regulated by NFκB. This result also shows that Fuc-liposome/NFκB decoy complexes can suppress the

activation of NFκB. As far as liver injury is concerned, serum ALT and AST levels were measured, because cytokine release from Kupffer cells has a cytotoxic effect on hepatocytes. ALT and AST levels were suppressed by Fuc-liposome/NFκB decoy complexes but not naked NFκB decoy (Fig. 5). This result also shows the Fuc-liposome/NFκB decoy complexes can suppress the activation of NFκB.

In a previous study, we demonstrated that intravenously injected bare cationic liposome/NFκB decoy complexes [22] and Man-liposome/NFκB decoy complexes [30] suppressed LPS-induced TNFα production in mice. Unlike Fuc-liposome complexes, after intravenous injection cationic liposome complexes rapidly and highly accumulated in the lung and then slowly accumulated in the liver (about 60% of dose/g tissue) [22]; therefore, liver accumulation of cationic liposome complexes was lower than that of Fuc-liposome complexes (Fig. 1). This could explain the fact that the production of TNFα could be attenuated by 20 μg NFκB decoy complexed with Fuc-liposomes but not by cationic liposomes (Fig. 4). As far as the characteristics of receptor recognition are concerned, both mannose receptor, which is expressed on sinusoidal endothelial cells and Kupffer cells, and fucose receptor, which is expressed on Kupffer cells, could recognize mannose and fucose. However, in our previous reports, intravenously injected mannosylated bovine serum albumin (BSA) was taken up by sinusoidal endothelial cells compared with Kupffer cells and fucosylated BSA was more selectively taken up Kupffer cells compared with sinusoidal endothelial cells [16,31]. This could explain the fact that 20 μg NFκB decoy complexed with Fuc-liposome more strongly reduced the serum level of TNFα than the same amount of NFκB decoy complexed with Man-liposomes (Fig. 4).

As far as the liver-specific delivery of NFκB decoy is concerned, Yoshida et al. [32] recently demonstrated that NFκB decoy was effectively transferred to Kupffer cells by fusigenic liposomes with hemagglutinating virus of Japan (HVJ liposomes) from the portal vein. Using this method, Ogushi et al. [33] demonstrated that NFκB decoy incorporated in HVJ liposomes effectively suppressed endotoxin-induced fatal liver injury in mice. However, intraportal injection is difficult in clinical situations because it needs a skillful surgical technique and increases the burden on the patient. Although intravenous injection is the simplest method, HVJ liposomes cannot accumulate in the liver following intravenous injection, because HVJ liposomes fuse to cells in a non-specific manner [32]. As a consequence, oligonucleotide is non-specifically delivered by HVJ liposomes to the lung, spleen and kidneys after intravenous injection [32]. In fact, Ogushi et al. [33] achieved a therapeutic effect only by intraportal injection of HVJ liposomes not by intravenous injection. Moreover, because Kupffer cells account for only 15% of the total liver cells [33], non-specific fusion of HVJ liposomes would cause an increase in the dose of NFκB decoy. Furthermore, preparing HVJ liposomes is complicated with irradiation being needed to remove viral toxicity and centrifugation to remove free HVJ [34].

5. Conclusion

In this study, novel Fuc-liposomes can be used as Kupffer cell-selective oligonucleotide carriers through recognition by the fucose receptors on Kupffer cells. Intravenously injected Fuc-liposome/NFκB decoy complexes effectively suppress LPS-induced TNFα and IFNγ production by suppression of NFκB transcription. Liver injury following to the cytokines production was also prevented Fuc-liposome/NFκB decoy complexes. Fuc-liposome/NFκB decoy complexes will prove to be a useful therapeutic tool for treating cytokine-related fatal inflammatory liver disease following administration by intravenous injection.

Acknowledgements

This work was supported in part by The Research Foundation for Pharmaceutical Sciences, Grants-in-Aid for Scientific Research from the Ministry of Education, Culture, Sports, Science, and Technology of Japan, and by Health and labor Sciences Research Grants for Research on Advanced Medical Technology from the Ministry of Health, Labor and Welfare of Japan, and The Research Foundation for Pharmaceutical Sciences and by Radioisotope Research Center of Kyoto University.

References

[1] Morrison DC, Ryan JL. Endotoxins and disease mechanisms. Annu Rev Med 1987;38:417–32.
[2] Ponnappa BC, Dey I, Tu GC, Zhou F, Aini M, Cao QN, et al. In vivo delivery of antisense oligonucleotides in pH-sensitive liposomes inhibits lipopolysaccharide-induced production of tumor necrosis factor in rats. J Pharmacol Exp Ther 2001;297:1129–36.
[3] Pahl HL. Activations and target genes of Rel/NF-κB transcription factors. Oncogene 1999;18:6853–66.
[4] Handa O, Naito Y, Takagi T, Shimozawa M, Kokura S, Yoshida N, et al. Tumor necrosis factor-alpha-induced cytokine-induced neutrophil chemoattractant-1 (CINC-1) production by rat gastric epithelial cells: role of reactive oxygen species and nuclear factor-κB. J Pharmacol Exp Ther 2004;309:670–6.
[5] Wrighton CJ, Hofer-Warbinek R, Moll T, Eytner R, Bach FH, de Martin R. Inhibition of endothelial cell activation by adenovirus-mediated expression of IκBa, an inhibitor of the transcription factor NF-κB. J Exp Med 1996;183:1013–22.
[6] Foxwell B, Browne K, Bondeson J, Clarke C, de Martin R, Brennan F, et al. Efficient adenoviral infection with IκBa reveals that macrophage TNFα production in rheumatoid arthritis is NF-κB dependent. Proc Natl Acad Sci USA 1998;95:8211–5.
[7] Bielinska A, Shivdasani RA, Zhang LQ, Nabel GJ. Regulation of gene expression with double-stranded phosphorothioate oligonucleotides. Science 1990;250:997–1000.
[8] Morishita R, Higaki J, Tomita N, Ogihara T. Application of transcription factor "decoy" strategy as means of gene therapy and study of gene expression in cardiovascular disease. Circ Res 1998;82:1023–8.
[9] Morishita R, Sugimoto T, Aoki M, Kida I, Tomita N, Moriguchi A, et al. In vivo transduction of cis element decoy against nuclear

factor-κB binding siteprevents myocardial infraction. Nat Med 1997; 3:894–9.
[10] Griesenbach U, Scheid P, Hillery E, de Martin R, Huang L, Geddes DM, et al. Anti-inflammatory gene therapy directed at the airway epithelium. Gene Ther 2000;7:306–13.
[11] Higuchi Y, Kawakami S, Nishikawa M, Yamashita F, Hashida M. Intracellular distribution of NFκB decoy and its inhibitory effect on TNFα production by LPS stimulated RAW 264.7 cells. J Control Release 2005;107:373–82.
[12] Kawakami S, Yamashita F, Nishida K, Nakamura J, Hashida M. Glycosylated cationic liposomes for cell-selective gene delivery. Crit Rev Ther Drug Carrier Syst 2002;19:171–90.
[13] Kawakami S, Sato A, Nishikawa M, Yamashita F, Hashida M. Mannose receptor-mediated gene transfer into macrophages using novel mannosylated cationic liposomes. Gene Ther 2000;7:292–9.
[14] Yamada M, Nishikawa M, Kawakami S, Hattori Y, Nakano T, Yamashita F, et al. Tissue and intrahepatic distribution and subcellular localization of a mannosylated lipoplex after intravenous administration in mice. J Control Release 2004;98:157–67.
[15] Hattori Y, Kawakami S, Suzuki S, Yamashita F, Hashida M. Enhancement of immune responses by DNA vaccination through targeted gene delivery using mannosylated cationic liposome formulations following intravenous administration in mice. Biochem Biophys Res Commun 2004;317:992–9.
[16] Opanasopit P, Nishikawa M, Yamashita F, Takakura Y, Hashida M. Pharmacokinetic analysis of lectin-dependent biodistribution of fucosylated bovine serum albumin: a possible carrier for Kupffer cells. J Drug Target 2001;9:341–51.
[17] Kuiper J, Brouwer A, Knook DL, van Berkel TJC. Kupffer and sinusoidal endothelial cells. In: Arias IM, Boyer JL, Fausto N, Jakoby WB, Schachter DA, Shafritz DA, editors. The liver: biology and pathobiology. 3rd ed. New York: Raven Press; 2001. p. 791–818.
[18] Kawakami S, Wong J, Sato A, Hattori Y, Yamashita F, Hashida M. Biodistribution characteristics of mannosylated, fucosylated, and galactosylated liposomes in mice. Biochim Biophys Acta 2000;1524: 258–65.
[19] Hattori Y, Suzuki S, Kawakami S, Yamashita F, Hashida M. The role of dioleoylphosphatidylethanolamine (DOPE) in targeted gene delivery with mannosylated cationic liposomes via intravenous route. J Control Release 2005;108:484–95.
[20] Yeeprae W, Kawakami S, Higuchi Y, Yamashita F, Hashida M. Biodistribution characteristics of mannosylated and fucosylated O/W emulsions in mice. J Drug Target 2005;13:479–87.
[21] Yang JP, Huang L. Overcoming the inhibitory effect of serum on lipofection by increasing the charge ratio of cationic liposome to DNA. Gene Ther 1997;4:950–60.
[22] Higuchi Y, Kawakami S, Oka M, Yamashita F, Hashida M. Suppression of TNFα production in LPS induced liver failure mice after intravenous injection of cationic liposome/NFκB decoy complex. Pharmazie 2006;61:144–7.
[23] Hardonk MJ, Dijkhuis FW, Hulstaert CE, Koudstaal J. Heterogeneity of rat liver and spleen macrophages in gadolinium chloride-induced elimination and repopulation. J Leukoc Biol 1992;52:296–302.
[24] Rüttinger D, Vollmar B, Wanner GA, Messmer K. In vivo assessment of hepatic alterations following gadolinium chloride-induced Kupffer cell blockade. J Hepatol 1996;25:960–7.
[25] Mas A, Rodés J. Fulminant hepatic failure. Lancet 1997;349:1081–5.
[26] Roland N, Wade J, Davalos M, Wendon J, Philpott-Howars J, Williams R. The system inflammatory response syndrome in acute liver failure. Hepatology 2000;32:734–9.
[27] Sands H, Gorey-Feret LJ, Cocuzza AJ, Hobbs FW, Chidester D, Trainor GL. Biodistribution and metabolism of internally ^{3}H-labeled oligonucleotides. I. Comparison of a phosphodiester and a phosphorothioate. Mol Pharmacol 1994;45:932–43.
[28] Brenner BM, Hostetter TH, Humes HD. Glomerular permselectivity: barrier function based on discrimination of molecular size and charge. Am J Physiol 1978;234:F455–60.
[29] Dzau VJ, Mann MJ, Morishita R, Kaneda Y. Fusigenic viral liposome for gene therapy in cardiovascular diseases. Proc Natl Acad Sci USA 1996;93:11421–5.
[30] Higuchi Y, Kawakami S, Oka M, Yabe Y, Yamashita F, Hashida M. Intravenous administration of mannosylated cationic liposome/$NF_{\kappa}B$ decoy complexes effectively prevent LPS-induced cytokine production in a murine liver model. FEBS Lett 2006;580:3706–14.
[31] Ogawara K, Hasegawa S, Nishikawa M, Hashida M. Pharmacokinetic evaluation of mannosylated bovine serum albumin as a liver cell-specific carrier: quantitative comparison with other hepatoropic ligands. J Drug Target 1999;6:349–60.
[32] Yoshida M, Yamamoto N, Uehara T, Terao R, Nitta R, Harada N, et al. Kupffer cell targeting by intraportal injection of the HVJ cationic liposome. Eur Surg Res 2002;34:251–9.
[33] Ogushi I, Iimuro Y, Seki E, Son G, Hirano T, Hada T, et al. Nuclear factor κB decoy oligonucleotides prevent endotoxin-induced fatal liver failure in a murine model. Hepatology 2003;38:335–44.
[34] Hirano T, Fujimoto J, Ueki T, Yamamoto H, Iwasaki T, Morisita R, et al. Persistent gene expression in rat liver in vivo by repetitive transfections using HVJ-liposome. Gene Ther 1998;5:459–64.

Available online at www.sciencedirect.com
ScienceDirect
Biomaterials 28 (2007) 1434–1442
Biomaterials
www.elsevier.com/locate/biomaterials

Small interfering RNA delivery to the liver by intravenous administration of galactosylated cationic liposomes in mice

Ayumi Sato[a], Motoki Takagi[a], Akira Shimamoto[a], Shigeru Kawakami[b], Mitsuru Hashida[b,*]

[a]*GeneCare Research Institute Co. Ltd., 200 Kajiwara, Kamakura, Kanagawa 247-0063, Japan*
[b]*Department of Drug Delivery Research, Graduate School of Pharmaceutical Sciences, Kyoto University, Sakyo-ku, Kyoto 606-8501, Japan*

Received 20 September 2006; accepted 7 November 2006
Available online 4 December 2006

Abstract

Although small interfering RNA (siRNA) is a potentially useful therapeutic approach to silence the targeted gene of a particular disease, its use is limited by its stability in vivo. For the liver parenchymal cell (PC)-selective delivery of siRNA, siRNA was complexed with galactosylated cationic liposomes. Galactosylated liposomes/siRNA complex exhibited a higher stability than naked siRNA in plasma. After intravenous administration of a galactosylated liposomes/siRNA complex, the siRNA did not undergo nuclease digestion and urinary excretion and was delivered efficiently to the liver and was detected in PC rather than liver non-parenchymal cells (NPC). Endogenous gene (Ubc13 gene) expression in the liver was inhibited by 80% when Ubc13–siRNA complexed with galactosylated liposomes was administered to mice at a dose of 0.29 nmol/g. In contrast, the bare cationic liposomes did not induce any silencing effect on Ubc13 gene expression. These results indicated that galactosylated liposomes/siRNA complex could induce gene silencing of endogenous hepatic gene expression. The interferon responses by galactosylated liposomes/siRNA complex were controlled by optimization of the sequence of siRNA. Also no liver toxicity due to galactosylated liposomes/siRNA complex was observed under any of the conditions tested. In conclusion, we demonstrated the hepatocyte-selective gene silencing by galactosylated liposomes following intravenous administration.

Keywords: Gene therapy; Liver; Liposome; Gene transfer

1. Introduction

RNA interference (RNAi) is induced by 21–25 nucleotide, double-stranded small interfering RNA (siRNA), which is incorporated into the RNAi-induced silencing complex (RISC) and is a guide for cleavage of the complementary target mRNA in the cytoplasm [1]. For therapeutic application, siRNA technology promises greater advantages over drugs currently on the market by offering new types of drugs that are easy to design and have a very high target selectivity, inhibiting a specific gene expression in the cytoplasm, and an expected low toxicity due to metabolism to natural nucleotide components by the endogenous cell systems [1–5]. However, siRNA therapeutics is hindered by the poor intracellular uptake and limited blood stability of siRNA and the current delivery methods to the target cells in vivo. When siRNA is administered in blood, it is readily digested by nuclease and eliminated from the renal glomeruli before reaching the diseased tissues. In order to achieve the therapeutic effect of siRNA at the target site, therefore, it is important to enhance the stability of siRNA in the blood circulation and to allow targeted delivery to the diseased area.

As far as in vivo selective gene delivery to hepatocytes is concerned, galactose has been shown to be a promising targeting ligand to hepatocytes (liver PCs) because the cells possess a large number of asialoglycoprotein receptors that recognize the galactose units on the oligosaccharide chains of glycoproteins or on the chemically synthesized galactosylated carriers [6]. In a series of investigations, we have studied liposomal systems to deliver plasmid DNA to hepatocytes in vivo and developed novel galactosylated cationic liposomes, including cationic charge linkers for

*Corresponding author. Tel.: +81 75 753 4525; fax: +81 75 753 4575.
E-mail address: hashidam@pharm.kyoto-u.ac.jp (M. Hashida).

0142-9612/$ - see front matter © 2006 Elsevier Ltd. All rights reserved.
doi:10.1016/j.biomaterials.2006.11.010

anionic compound binding and galactose moieties as a targetable ligand for PC. The galactosylated cationic liposomes are composed of galactosylated cholesterol derivatives, cholesten-5-yloxy-*N*-(4-((1-imino-2-D-thiogalactosylethyl)amino)alkyl)formamide (Gal-C4-Chol) and a neutral lipid. Based on the optimization of the physicochemical properties of the galactosylated liposomes/plasmid DNA complexes [7–10], we have succeeded in developing a hepatocyte-selective gene targeting system. Ma et al. [11] have reported that cationic liposomes enhance siRNA-mediated interferon (IFN) responses by the activation of STAT1 in mice. In contrast, naked siRNA did not induce the IFN responses. Recently, Zhang and Wang have reported that the siRNA of hepatitis C is a novel strategy for the treatment of this disease in vitro [12,13]. Since IFN can be used for the treatment of virus hepatitis, these observations prompted us to investigate whether a galactosylated liposomes/siRNA complex could achieve both gene silencing in hepatocytes and IFN induction after intravenous administration.

In the present study, siRNA delivery to the liver by intravenous administration of galactosylated liposomes was examined. Results are compared with naked siRNA (conventional injection or hydrodynamic injection) and cationic liposomes/siRNA complex.

2. Materials and methods

2.1. Materials

Dioleoylphosphatidylethanolamine (DOPE), 3β[*N*-(*N'*,*N'*-dimethylaminoethane)carbomyl]cholesterol (DC-Chol), L-α-phosphatidylcholine, hydrogenated from chicken egg (Egg PC) and 1,2-dioleoyl-*sn*-glycero-3-phosphocholine (DOPC) were purchased from Avanti Polar-Lipids Inc. (Alabaster, AL). The preparation of Gal-C4-Chol has been described previously [14]. siRNAs (21 mer) with 3′-dTdT overhangs were chemically synthesized by Nippon EGT Co. Ltd. (Toyama, Japan). The siRNA sequences are shown in Table 1. The Ubc13 siRNA modified with Alexa Fluor 546 or fluorescein at the 3′ termini of the sense strand was synthesized by QIAGEN K.K. (Tokyo, Japan).

2.2. Preparation of liposomes

A mixture of Gal-C4-Chol and DOPE with a molar ratio of 3:2 was dissolved in chloroform, vacuum-desiccated, and resuspended in sterile 5% dextrose solution. The suspension was sonicated and the resulting liposomes were extruded 10 times through double-stacked 100 nm polycarbonate membrane filters. Cationic liposomes and siRNA was complexed at a charge ratio (−:+) of 1.0:2.3 for cell-selective delivery [7]. The particle size and zeta potential of the liposomes were measured using a Nano ZS apparatus (Malvern Instruments Ltd., Malvern, WR, UK). All other liposomes, Gal-C4-Chol, cholesterol, and DOPE (molar ratio = 1:1:1), Gal-C4-Chol and Egg PC (molar ratio = 3:2) and Gal-C4-Chol and DOPC (molar ratio = 3:2) were prepared by a similar procedure.

2.3. Stability of galactosylated liposomes/siRNA complex in mouse plasma

For siRNA stability in blood plasma, a solution (30 μl) of 150 pmol siRNA (Alexa Fluor 546-labeled siRNA: no labeled siRNA = 1:4) complexed with the galactosylated liposomes (Gal-C4-Chol/DOPE liposomes) was mixed with 270 μl fresh mouse plasma to give a final plasma concentration of 90%. After incubation at 37 °C for specific time periods, aliquots (20 μl) were collected and mixed with 10 μl 9% sodium dodecyl sulfate solution. The siRNAs were extracted from the reaction mixtures with phenol/chloroform/isoamyl alcohol (25:24:1). The siRNAs were electrophoresed on 4–20% polyacrylamide gel (Tefco Inc., Tokyo, Japan) and visualized with a fluorescence image analyzer, FMBIO II (Hitachi Software Engineering Co. Ltd., Tokyo, Japan).

2.4. Stability of galactosylated liposomes/siRNA complex in vivo

The animal experiments in the present study were approved by the Animal Research Committee of the GeneCare Research Institute Co. Ltd. Male ICR mice (age 5 weeks) were purchased from CLEA Japan Inc. (Tokyo, Japan). For the in vivo stability study of siRNA, Alexa Fluor 546-labeled siRNA and unlabeled siRNA were mixed in a 1:4 ratio. The galactosylated liposomes (Gal-C4-Chol/DOPE liposomes)/siRNA complex solution was administered intravenously (0.1 nmol siRNA/10 μl/g) and blood samples were collected from each mouse. Then 20 μl of each blood sample was added to 10 μl 9% sodium dodecyl sulfate solution. The siRNAs in the blood samples were extracted and electrophoresed by the procedures described above.

2.5. Biodistribution of galactosylated liposomes/siRNA complex in mice

The galactosylated liposomes (Gal-C4-Chol/DOPE liposomes) and fluorescein-labeled siRNA complex solution was injected intravenously into mice (0.1 nmol siRNA/10 μl/g). At 5 and 60 min following administration, the organs were harvested and rinsed with saline. The fluorescein-labeled siRNA in the organs was visualized in a fluorescence image analyzer, FMBIO II.

2.6. Detection of siRNA in liver cells

The liposomes and fluorescein-labeled siRNA complex solution was injected intravenously into mice (0.1 nmol siRNA/10 μl/g). At 48 h post-injection of the liposomes/siRNA complex, the liver was removed rinsed with saline, frozen in liquid nitrogen and mounted for cryostat sectioning. Slides were viewed under a fluorescence microscope.

Table 1
Sequence of siRNAs

siRNA	Sequence of sense strand
Ubc13–siRNA	5′-GUACGUUUCAUGACCAAAA-dTdT-3′
Non-specific control siRNA (NS-siRNA)	5′-UUCUCCGAACGUGUCACGU-dTdT-3′
siRNA1	5′-GUUCAGACCACUUCAGCUU-dTdT-3′
siRNA2	5′-GCUUGAAACUAUUAACGUA-dTdT-3′

2.7. Gene silencing effect in various organs

Liposomes and Ubc13 siRNA complex solution were injected intraportally or intravenously into mice at a normal pressure (0.18 nmol siRNA/18 μl/g). As for the hydrodynamic injection, Ubc13 siRNA were injected intravenously at a volume of 1.6 ml siRNA solution [15–17]. At 48 h following administration, the organs were removed and rinsed with saline. The total RNAs were extracted from the organs using an RNeasy Mini Kit (Qiagen) according to the manufacturer's protocol. RT-PCR analyses were carried out using an ABI Prism 7000 Sequence Detection System and Taqman probes and primers (Applied Biosystems, Foster City, CA). The glyceraldehyde-3-phosphate dehydrogenase gene (GAPDH) was used as the standard.

2.8. Measurement of IFN, aspartate aminotransferase (AST) and alanine aminotransferase (ALT) in mouse blood

Groups of three mice were intravenously injected with galactosylated liposomes (Gal-C4-Chol/DOPE liposomes)/siRNA (0.18 nmol siRNA/g) complex. At 5 h following the administration, blood samples were collected and the IFN-α and IFN-γ levels measured by ELISA. Mouse IFN-α and IFN-γ ELISA kits were purchased from PBL Biomedical Laboratories (Piscataway, NJ) and GE Healthcare Bio-Sciences Co. (Piscataway, NJ), respectively. The measurements were performed according to the manufacturer's instructions.

For detection of AST and ALT, mouse blood samples were collected at 5 and 20 h following administration. The aminotransferase activities were measured using a Transaminase CII-Test Wako kit (Wako Pure Chemical Industries Ltd., Tokyo, Japan) according to manufacturer's instructions.

3. Results

3.1. Physicochemical properties of galactosylated liposomes/siRNA complex

The particle sizes of the galactosylated liposomes were 50.1 ± 3.6 nm and the zeta potentials were 47.9 ± 0.7 mV (Table 2). Also, the particle sizes of the galactosylated liposomes complexed with siRNA were 75.3 ± 5.8 nm and the zeta potentials were 35.8 ± 1.8 mV. The particle sizes of the galactosylated liposomes/siRNA complex were larger and the zeta potentials were lower than those of the galactosylated liposomes, suggesting that the galactosylated liposomes and siRNA form complexes by their electrostatic interaction.

3.2. Stability of siRNA in mouse plasma

Naked siRNA underwent almost 90% digestion by nuclease within 3 h at 37 °C (Fig. 1). Under the same conditions, the siRNA complexed with galactosylated liposomes remained intact at 30 h. This showed that the galactosylated liposomes conferred a highly protective effect against nuclease as far as siRNA was concerned. Also, this result indicated that the ionic interaction between galactosylated liposomes and siRNA is unaffected by various ionic component, i.e. lipids, proteins, and polysaccharides in plasma.

3.3. Delivery of galactosylated liposomes/siRNA complex to liver

Fig. 2 shows the amount of intact siRNA in the blood circulation after intravenous administration. Naked siRNA was eliminated from the blood within 5 min and excreted in urine. In contrast, the galactosylated liposomes prolonged the circulation of siRNA in the mouse bloodstream compared with naked siRNA. The siRNA was detected in the bloodstream but not in the urine 60 min following injection. This result suggests that the galactosylated liposomes/siRNA complex is not digested by nuclease and eliminated via the renal glomeruli. Furthermore, the complex might be slowly distributed in some organs instead of remaining in the circulating blood.

Next, we investigated the biodistribution of siRNA in the heart, lung, liver, spleen and kidney at 5 and 60 min after administration of the galactosylated liposomes/siRNA complex to mice. The siRNA was detected in the liver, lung and kidney compared with untreated mice at 5 min (Fig. 3). Despite elimination of siRNA from the bloodstream at 60 min, the siRNA remained in the liver and lung. These results show that the siRNA disappearing from the bloodstream is delivered to the liver by galactosylated liposomes formulations.

3.4. Cellular localization of siRNA in liver

Fig. 4 shows images of frozen sections of livers under fluorescence microscopy. In the galactosylated liposomes (Gal-C4-Chol/DOPE)/siRNA complex-injected mice, fluorescein-labeled siRNA was detected abundantly in liver cells and the fluorescence intensity was higher than that in the mice injected with cationic liposomes (DC-Chol/DOPE)/siRNA complex. In construct, there was hardly any siRNA in liver cells when cationic liposomes/siRNA complex was used. Considering that hepatocytes account for almost 80% of the total liver volume by PC, these results indicate that galactosylated liposomes/siRNA complex is incorporated efficiently into PC by the galactose ligand of galactosylated liposomes.

Table 2
Particle size and zeta potential of galactosylated liposomes and its complex

Formulations	Particle size (nm)	ζ potential (mV)
Galactosylated liposomes (Gal-C4-Chol/DOPE)	50.1 ± 3.6	47.9 ± 0.7
Galactosylated liposomes/siRNA complex	75.3 ± 5.8	35.3 ± 1.8

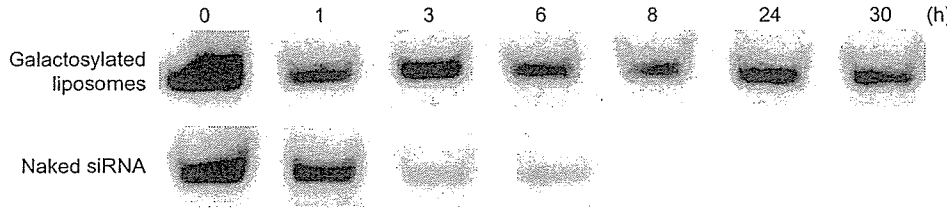

Fig. 1. Stability of galactosylated liposomes/siRNA complex in mouse plasma. Alexa fluor 546-labeled siRNA and unlabeled siRNA mixture (1:4 mol/mol) was complexed with galactosylated liposomes (Gal-C4-Chol/DOPE) and incubated in 90% plasma at 37 °C for 1, 3, 6, 8, 24, and 30 h. The remaining siRNAs were separated by gel electrophoresis and fluorescence labeled siRNAs were detected by image analysis. Naked siRNA was used as a negative control.

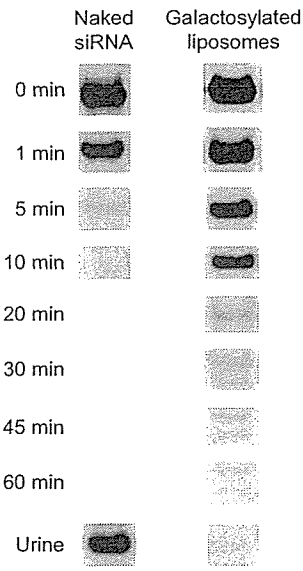

Fig. 2. Stability of siRNA complexed with galactosylated liposomes in blood circulation after intravenous administration in mice. siRNA (Alexa fluor 546-siRNA and unlabeled siRNA = 1:4) complexed with galactosylated liposomes (Gal-C4-Chol/DOPE) was administered to mice intravenously. A total of 40 μl of blood and urine was collected at each time point (urine: 60 min) and the remaining siRNAs were determined by gel electrophoresis and image analysis. Naked siRNA was used as a negative control.

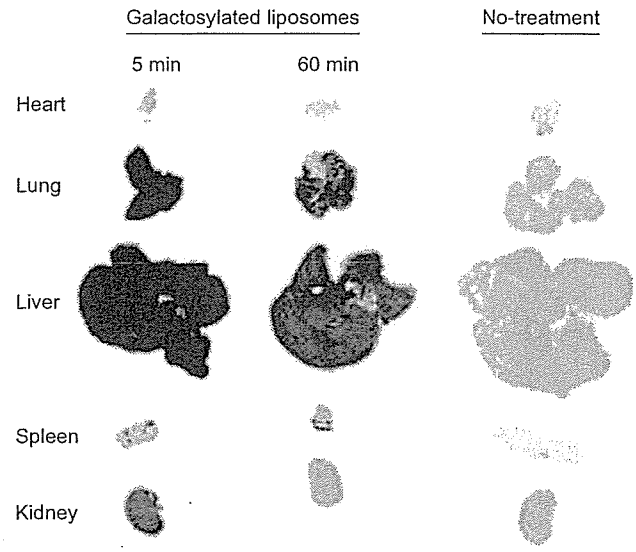

Fig. 3. Biodistribution characteristics of siRNA in tissues after intravenous administration of galactosylated liposomes/fluorescein-labeled siRNA complex in mice. Fluorescein-labeled siRNA complexed with Gal-C4-Chol/DOPE liposomes was administered to mice intravenously. At 5 and 60 min following administration, mice were sacrificed and lung, liver, kidney, spleen and heart were collected. The remaining siRNAs in organs were detected by image analysis. The control is organs from an untreated mouse.

3.5. Silencing of endogenous gene expression in liver

Since siRNA was delivered to liver by galactosylated liposomes after systemic injection into mice, we examined the ability of the siRNA to silence endogenous gene expression in liver. We used the siRNA corresponding Ubc13 gene, which is known to be expressed in various organs constitutively and ubiquitously, and confirmed that the Ubc13 gene is expressed in the mouse lung, liver, kidney, spleen and heart using RT-PCR (data not shown). The Ubc13–siRNA had the ability to suppress 80% of Ubc13 gene expression in HepG2 cells, human hepatic carcinoma, at 1 nm under the culture conditions used (data not shown).

To investigate if Ubc13–siRNA suppresses the expression of Ubc13 mRNA in liver, we administered Ubc13–siRNA into the portal vein of mice using galactosylated liposomes (Gal-C4-Chol/DOPE liposomes) or cationic liposomes (DC-Chol/DOPE liposomes). Although, the silencing effect of the Ubc13 gene expression in liver was observed with each complex after intraportal administration (Fig. 5A), the galactosylated liposomes/siRNA complex exhibited greater suppression of the expression of Ubc13 gene. The in vivo RNAi activity of the Ubc13–siRNA was validated by this result.

The gene suppression effects were also compared with those following hydrodynamic injection [15–17] of Ubc13–siRNA. After intravenous administration, the galactosylated liposomes/Ubc13–siRNA complex effectively suppressed the expression of Ubc13 gene in liver and lung as compared with hydrodynamic injection at 48 h after the injections (Fig. 5B). Notably, the Ubc13 gene expression in liver was suppressed by more than 60% with galactosylated liposomes while in the case of the cationic liposomes complex, no RNAi effects were observed in any organs. These results indicated that galactosylated

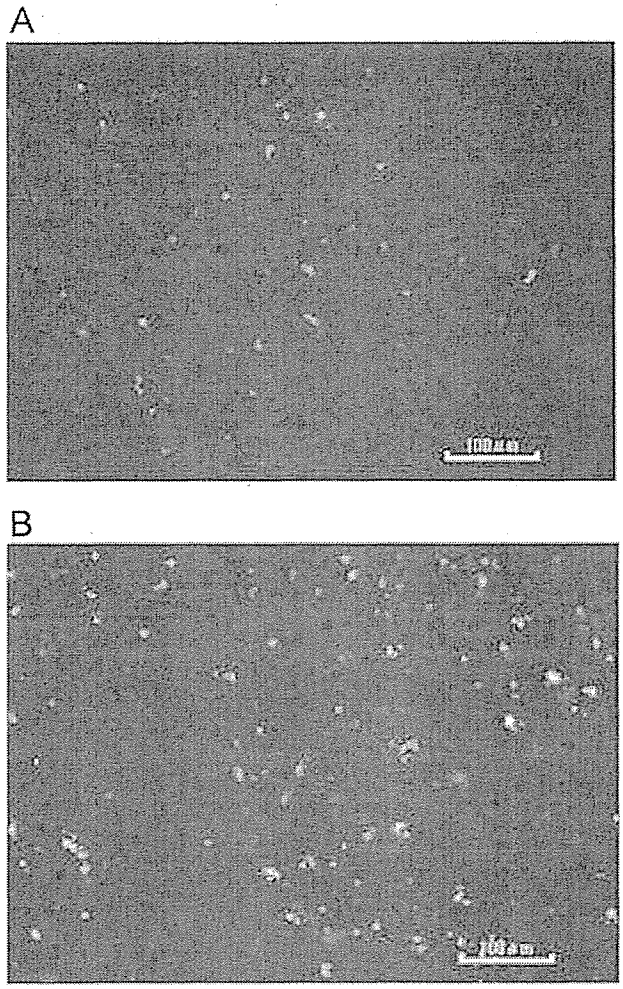

Fig. 4. Cellular localization of siRNA in liver after intravenous administration of galactosylated liposomes/fluorescein-labeled siRNA complex in mice. Fluorescein-labeled siRNA was complexed with cationic liposomes (A) or galactosylated liposomes (B). At 48 h after administration, the livers were removed and mounted for cryostat sectioning. Slides were viewed under a fluorescence microscope.

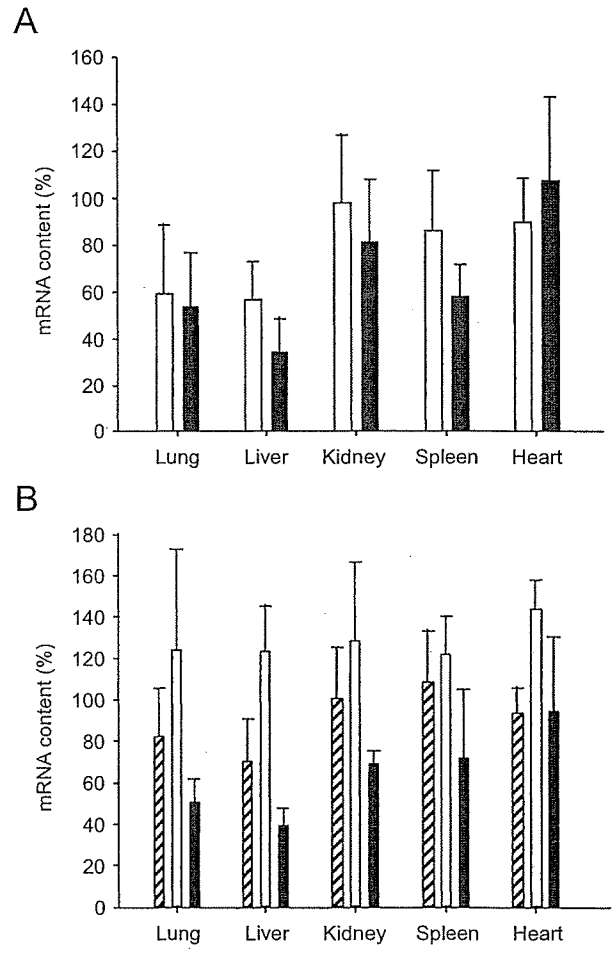

Fig. 5. Suppression of gene expression by galactosylated liposomes/siRNA complex in various organs in mice. Ubc13–siRNA complexed with cationic liposomes (white bar) or galactosylated liposomes (black bar) was injected intraportally (A) or intravenously (B) into mice. Also, Ubc13–siRNA was administered by the hydrodynamic injection method (hatched bar). At 48 h after administration, lung, liver, kidney, spleen and heart were collected. The total RNAs were extracted from the organs and subjected to RT-PCR analysis. Ubc13 mRNA levels in mice given injections of NS-siRNA complexed with respective liposomes, were taken as 100%. Groups of three mice were used and their average expressions of Ubc13 gene are illustrated.

liposomes have a greater potential as a hepatic targeting delivery carrier for siRNA even following intravenous administration.

3.6. Effect of siRNA dose and lipid composition of galactosylated liposomes on gene silencing in liver

We showed that galactosylated liposomes/Ubc13–siRNA complex induces silencing of Ubc13 gene expression in a dose-dependent manner. When 0.1 nmol/g siRNA was administered to mice, no silencing effect was observed (Fig. 6A). However, suppression of Ubc13 gene expression in liver occurred at over 0.18 nmol/g and suppression was observed in other organs at 0.29 and 0.36 nmol/g. The most liver-selective silencing effects were obtained at 0.18 nmol/g. Also, the silencing effect in liver by injection of 0.36 nmol/g siRNA was not greater than that using 0.29 nmol/g. These results showed that the range of siRNA dose-dependence is from 0.18 to 0.36 nmol/g when galactosylated liposomes are used.

To evaluate the lipid composition of galactosylated liposomes, we prepared galactosylated liposomes with Gal-C4-Chol and some neutral lipids, cholesterol, Egg PC and DOPC instead of DOPE. Except for Gal-C4-Chol/Egg PC, these liposomes complexed with siRNA at a charge ratio (−:+) of 1.0:2.3, and Gal-C4-Chol/Egg PC liposomes were prepared at a charge ratio (−:+) of 1.0:1.5. All galactosylated liposomes successfully induced gene silencing of Ubc13 in liver by more than 50% when 0.18 nmol/g siRNA was systemically administered to mice (Fig. 6B). Among the galactosylated liposomes tested, Gal-C4-Chol/DOPE

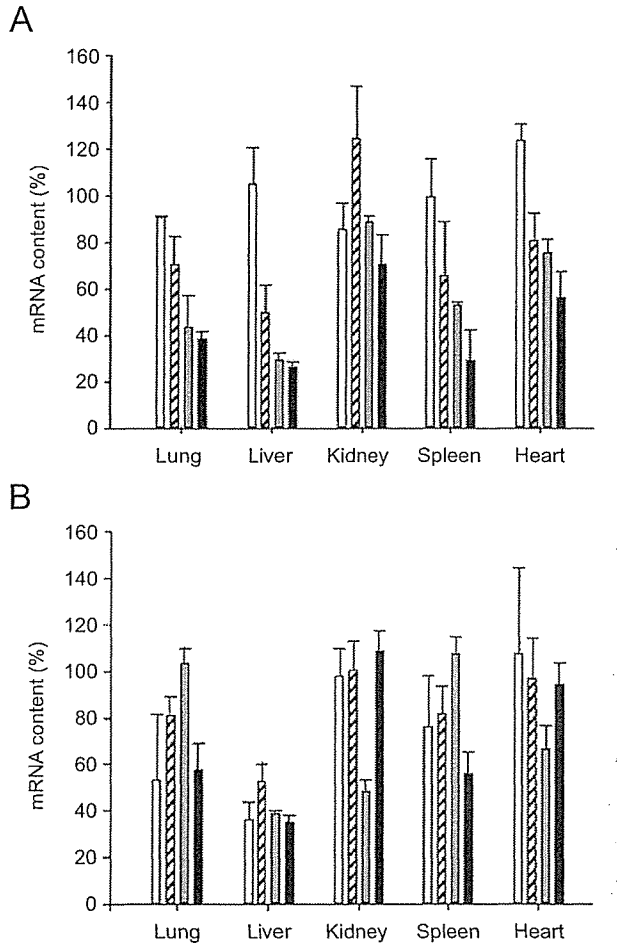

Fig. 6. Effect of siRNA dose (A) and lipid composition of galactosylated liposomes (B) on gene silencing in mice. Galactosylated liposomes (Gal-C4-Chol/DOPE)/Ubc13–siRNA complex was intravenous injected into mice ($N = 3$) at an siRNA dose of 0.10 (white bar), 0.18 (hatched bar), 0.29 (gray bar), or 0.36 (black bar) nmol/g. Ubc13–siRNA complexed with Gal-C4-Chol/DOPE liposomes (white bar), Gal-C4-Chol/cholesterol/DOPE liposomes (hatched bar), Gal-C4-Chol/EggPC liposomes (gray bar) or Gal-C4-Chol/DOPC liposomes (black bar) was intravenous injected into mice ($N = 3$) (B). At 48 h after intravenous administration, organs were collected and subjected to RT-PCR analysis. Ubc13 mRNA levels of mice injected with NS-siRNA complexed with respective liposomes were taken as 100%.

liposomes were the most effective and liver-selective. The silencing effect produced by Gal-C4-Chol/cholesterol/DOPE liposomes in liver was less than that produced by Gal-C4-Chol/DOPE liposomes. These results provide the evidence that Gal-C4-Chol is the most effective means of producing gene silencing with galactosylated liposomes in the liver.

3.7. Immune responses in liver by galactosylated liposomes/siRNA complex

Recent investigations have shown that cationic liposomes/siRNA complex induces IFN responses in mice [11,18–20]. To determine the IFN response by galactosylated liposomes/siRNA complex, we measured the induction level of IFN-α and IFN-γ as type I and type II IFN responses by ELISA. Galactosylated liposomes (Gal-C4-Chol/DOPE liposomes) were complexed with three kinds of siRNAs (NS-siRNA, siRNA1 and siRNA2, shown in Table 1) and injected intravenously into mice. As shown in Fig. 7, the galactosylated liposomes/siRNA complexes and galactosylated liposomes alone, except for siRNA1, failed to induce IFN-α and IFN-γ at 5 h after administration. In contrast, galactosylated liposomes/siRNA1 complex induced a higher level of IFN-α and, especially IFN-γ, compared with galactosylated liposomes/NS-siRNA complex and siRNA2 complex. It has been reported that the immune responses by siRNA are dependent on the sequence of the siRNA [21–23]. These results suggested that IFN responses are not caused by galactosylated liposomes and depend on the siRNA sequence.

The galactosylated liposomes/siRNA complex did not increase ALT and AST levels in mouse serum compared with the levels in untreated mice (Fig. 8). These results indicate that administration of galactosylated liposomes/siRNA complexes do not induce hepatitis in mice even when galactosylated liposomes/siRNA1 complex is injected.

4. Discussion

In this study, we showed that siRNA could be delivered to PC by carrying out experiments involving biodistribution and cellular localization in the liver with galactosylated liposomes (Figs. 3 and 4). Furthermore, we confirmed that endogenous hepatic gene (Ubc13 gene) mRNA is markedly reduced in liver by more than 60% with the galactosylated liposomes/siRNA (Ubc13–siRNA) complex (Figs. 5 and 6). Considering that PC account for about 80% of the total number of liver cells, it is suggested that Ubc13 mRNA in PC is degraded by galactosylated liposomes/siRNA complex. All of these data provide evidence that the inhibition of endogenous gene expression could be accompanied by an efficient uptake of siRNA by PC in liver.

To date, there has been little published information about formulations for the in vivo targeted delivery of siRNA and/or oligonucleotides. In order to optimize the in vivo delivery of siRNA by galactosylated liposomes, the characteristics of galactosylated liposomes as an siRNA delivery system were evaluated based on (i) the route of administration (intraportal vs. intravenous), (ii) the dose of siRNA, and (iii) the composition of neutral helper lipid. Interestingly, an RNAi effect in liver by galactosylated liposomes/siRNA complexes was observed irrespective of the route of administration (Fig. 5) and the type of neutral lipid (DOPE, Egg PC, and DOPC) in the galactosylated liposomes (Fig. 6). These differences between siRNA and plasmid DNA are unclear, and this event may be caused by a different mechanism in the cell between the RNAi effect

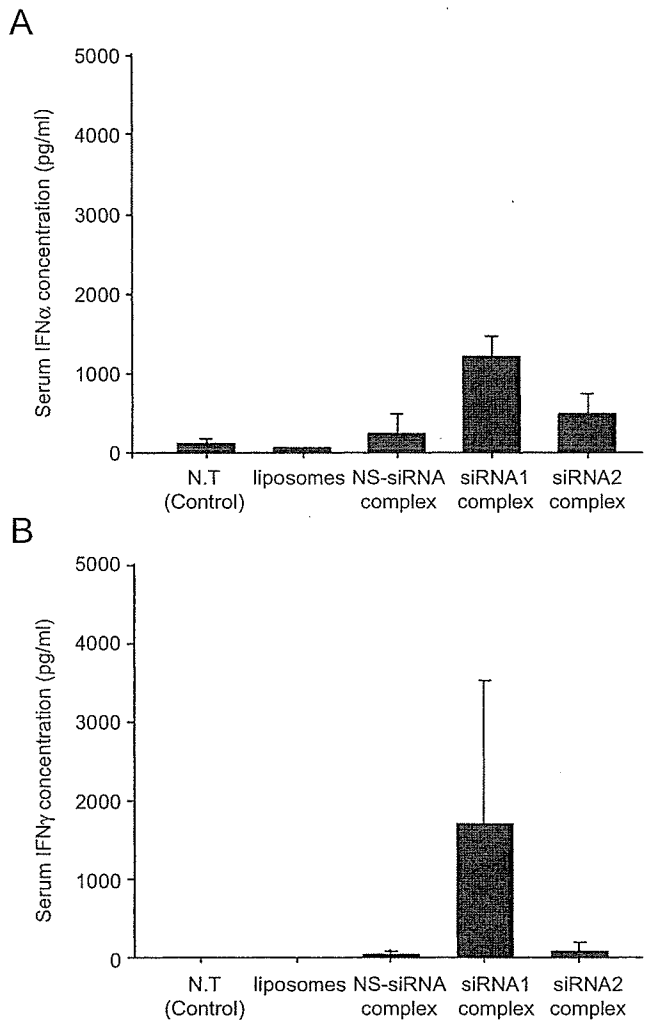

Fig. 7. Serum IFN-α (A) and IFN-γ (B) concentrations after intravenous administration of galactosylated liposomes/siRNA complex in mice. Groups of three mice were intravenously injected with galactosylated liposomes (Gal-C4-Chol/DOPE) complexed with NS-siRNA, siRNA1 and siRNA2 (5 nmol siRNA/mouse), respectively. At 5 h following administration, blood samples were collected and INF-α levels measured by ELISA. N.T. represents non-treated mice.

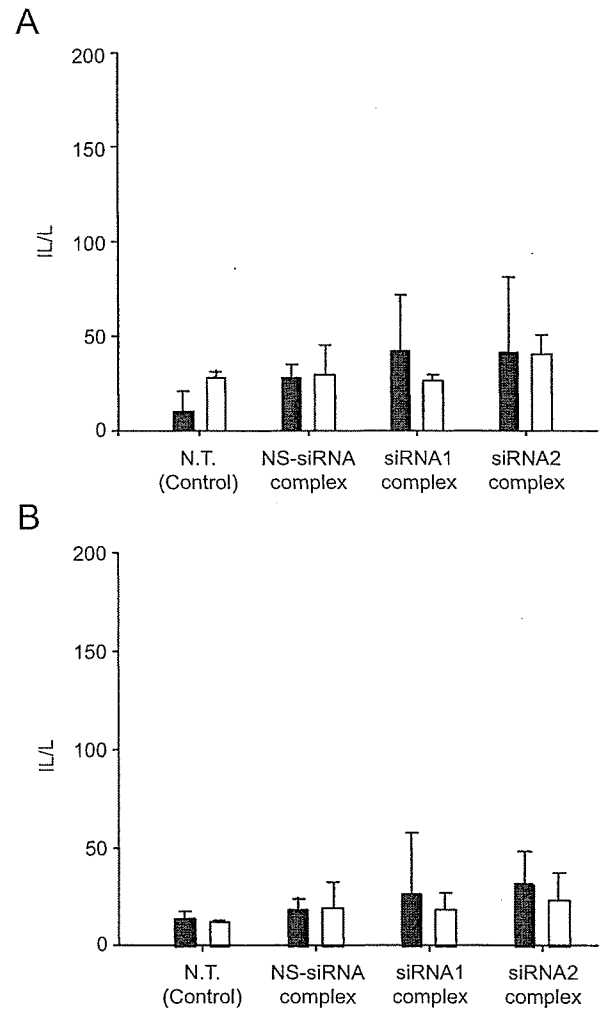

Fig. 8. Serum ALT (A) and AST (B) levels after intravenous administration of galactosylated liposomes/siRNA complex. Groups of three mice were intravenously injected with galactosylated liposomes (Gal-C4-Chol/DOPE) complexed with NS-siRNA, siRNA1 and siRNA2 (5 nmol siRNA/mouse), respectively. Blood samples were collected at 5 (black bar) and 20 h (white bar) following administration and AST and ALT levels were measured. One IU of enzyme activity represents 1 μmol substrate per 1 min at 25 °C.

by siRNA and the gene expression by plasmid DNA. This might be due to the difference in the mean diameters of the galactosylated liposomes/siRNA complex (about 75 nm) and the galactosylated lipoplex (about 100–150 nm), because we previously demonstrated that the mean diameters of galactosylated lipoplex markedly affected the transfection efficacy in PC in vivo [10].

There are three problems involved in the delivery of plasmid DNA into the cell nucleus from outside the cell and obtaining gene expression in the nucleus: the first involves approaching the cell membrane, the second involves escaping from the endosomes and the third is the passage through the membrane of the nucleus. In the case of siRNA delivery, since RNAi systems operate in cytoplasm, only two steps are needed. Moreover, siRNA has a low molecular weight and a low effective concentration in cells, compared with plasmid DNA. The characteristics of siRNA involve enhanced potential as a delivery system of galactosylated liposomes which might make it easier to design an siRNA delivery system.

It is known that IFN responses are induced by single- and double-stranded RNA associated with viral infection in mammalian cells and when siRNA is transfected into cells it is also able to stimulate type I IFN-α [24]. Furthermore, siRNA complexed with cationic liposomes containing cationic lipids (DOTAP; 1,2-dioleyl-3-trimetylammoniumpropane) activates siRNA-mediated type I and II IFN responses in mice [11]. To develop an siRNA hepatocyte-selective delivery system without side-effects, it is important to avoid the immune responses. Therefore, we

evaluated the levels of IFN-α and IFN-γ, as types I and II IFN responses, in mouse serum to investigate the toxicity of the galactosylated liposomes/siRNA complex. As shown in Fig. 7, the galactosylated liposomes/siRNA complex induced IFN-α and IFN-γ depending on the sequence of siRNA when given intravenously to mice. This is consistent with recent reports about siRNA/cationic liposomes complex [18–20]. These observations lead us to believe that IFN-γ induction by galactosylated liposomes/siRNA complex can be control by optimization of the siRNA sequence. Combination therapy using IFN-γ and IFN-α and gene silencing by siRNA would be more effective for the treatment of some viral diseases i.e., hepatitis C. Therefore, further studies are needed to analyze the relationship between IFNs induction and the sequence of siRNA for designing rational treatments involving the injection of galactosylated liposomes/siRNA complex.

As shown in Fig. 8, none of the galactosylated liposomes/siRNA complexes cause significant hepatitis in mice even although the galactosylated liposomes/siRNA1 complex induced IFN-γ. It has been reported that intravenous injection of cationic liposomes/plasmid DNA complex induces hepatic toxicity [25–27]. However, the hepatic toxicity due to cationic liposomes/plasmid DNA complex is induced by proinflammatory cytokines secreted from macrophages following recognition of the CpG motif in plasmid DNA [21]. In contrast, in the case of siRNA systems, IFN responses can be controlled by optimization of the siRNA sequence (Fig. 7). Therefore, these observations suggest that siRNA may be safer than plasmid DNA when delivered by (galactosylated) cationic liposomes.

Recently, Morrissey et al. [22] reported the sustained circulation in the blood of a formulation of chemically modified siRNA employing polyethylene glycol (PEG)-modified liposomes. They demonstrated that lipid-encapsulated siRNA against HBV (hepatitis B virus) was efficiently delivered to mouse liver and reduced the HBV DNA titer in vivo. Also, it has been reported that siRNA can silence the disease target apolipoprotein B (ApoB) in the liver when administered systemically to non-human primates (cynomolgus monkeys) with PEG-modified liposomes [23]. Other reports have also described that siRNA complexed with liposomes induces RNAi effects in liver [28,29]. However, hepatocyte-selective targeting delivery systems for siRNA have not been reported yet. We suggest that the use of galactosylated liposomes for siRNA delivery is more effective in lowering the dose and increasing the effect of siRNA against HBV and apoB. Therefore, galactosylated liposomes have great potential as a therapeutic application of siRNA for the treatment of liver diseases without significant side-effects following intravenous administration.

5. Conclusion

Our results showed that siRNA could be delivered to PC in experiments involving biodistribution and cellular localization in liver with galactosylated liposomes but not with cationic liposomes when administrated via the tail vein of mice. Furthermore, we confirmed that endogenous hepatic gene (Ubc13 gene) mRNA is markedly reduced in the liver, by more than 60%, when the galactosylated liposomes/siRNA (Ubc13–siRNA) complex is used. By the optimization of RNA sequences of the galactosylated liposomes/siRNA complexes, type I IFN responses, which are induced by single- and double-stranded RNA associated with viral infection in mammalian cells, can be induced and/or controlled. In addition, the galactosylated liposomes/siRNA complex did not cause any significant hepatitis via cytokine production in mice. These observations suggest that galactosylated liposomes are an efficient carrier of siRNA for hepatocyte-selective gene silencing following intravenous administration.

Acknowledgments

This work was supported in part by Grants-in-aid for Scientific Research from the Ministry of Education, Culture, Sports, Science, and Technology of Japan, and by Health and Labour Sciences Research Grants for Research on Advanced Medical Technology from the Ministry of Health, Labour and Welfare of Japan.

References

[1] Dorsett Y, Tuschl T. siRNAs: applications in functional genomics and potential as therapeutics. Nat Rev Drug Discov 2004;3(4):318–29.
[2] Lu PY, Xie FY, Woodle MC. siRNA-mediated antitumorigenesis for drug target validation and therapeutics. Curr Opin Mol Ther 2003;5(3):225–34.
[3] Ichim TE, Li M, Qian H, Popov IA, Rycerz K, Zheng X, et al. RNA interference: a potent tool for gene-specific therapeutics. Am J Transplant 2004;4(8):1227–36.
[4] Karagiannis TC, El-Osta A. RNA interference and potential therapeutic applications of short interfering RNAs. Cancer Gene Ther 2005;12(10):787–95.
[5] Ryther RC, Flynt AS, Phillips 3rd JA, Patton JG. siRNA therapeutics: big potential from small RNAs. Gene Ther 2005;12(1):5–11.
[6] Kawakami S, Yamashita F, Nishida K, Nakamura J, Hashida M. Glycosylated cationic liposomes for cell-selective gene delivery. Crit Rev Ther Drug Carrier Syst 2002;19(2):171–90.
[7] Kawakami S, Fumoto S, Nishikawa M, Yamashita F, Hashida M. In vivo gene delivery to the liver using galactosylated cationic liposomes. Pharm Res 2000;17(3):306–13.
[8] Fumoto S, Kawakami S, Ito Y, Shigeta K, Yamashita F, Hashida M. Enhanced hepatocyte-selective in vivo gene expression by stabilized galactosylated liposome/plasmid DNA complex using sodium chloride for complex formation. Mol Ther 2004;10(4):719–29.
[9] Fumoto S, Kawakami S, Shigeta K, Higuchi Y, Yamashita F, Hashida M. Interaction with blood components plays a crucial role in asialoglycoprotein receptor-mediated in vivo gene transfer by galactosylated lipoplex. J Pharmacol Exp Ther 2005;315(2):484–93.
[10] Higuchi Y, Kawakami S, Fumoto S, Yamashita F, Hashida M. Effect of the particle size of galactosylated lipoplex on hepatocyte-selective gene transfection after intraportal administration. Biol Pharm Bull 2006;29(7):1521–3.

[11] Ma Z, Li J, He F, Wilson A, Pitt B, Li S. Cationic lipids enhance siRNA-mediated interferon response in mice. Biochem Biophys Res Commun 2005;330(3):755–9.
[12] Zhang T, Lin RT, Li Y, Douglas SD, Maxcey C, Ho C, et al. Hepatitis C virus inhibits intracellular interferon alpha expression in human hepatic cell lines. Hepatology 2005;42(4):819–27.
[13] Wang Y, Kato N, Jazag A, Dharel N, Otsuka M, Taniguchi H, et al. Hepatitis C virus core protein is a potent inhibitor of RNA silencing-based antiviral response. Gastroenterology 2006;130(3):883–92.
[14] Kawakami S, Yamashita F, Nishikawa M, Takakura Y, Hashida M. Asialoglycoprotein receptor-mediated gene transfer using novel galactosylated cationic liposomes. Biochem Biophys Res Commun 1998;252(1):78–83.
[15] Liu F, Song Y, Liu D. Hydrodynamics-based transfection in animals by systemic administration of plasmid DNA. Gene Ther 1999;6(7): 1258–66.
[16] Song E, Lee SK, Wang J, Ince N, Ouyang N, Min J, et al. RNA interference targeting Fas protects mice from fulminant hepatitis. Nat Med 2003;9(3):347–51.
[17] Matsui Y, Kobayashi N, Nishikawa M, Takakura Y. Sequence-specific suppression of mdr1a/1b expression in mice via RNA interference. Pharm Res 2005;22(12):2091–8.
[18] Hornung V, Guenthner-Biller M, Bourquin C, Ablasser A, Schlee M, Uematsu S, et al. Sequence-specific potent induction of IFN-α by short interfering RNA in plasmacytoid dendritic cells through TLR7. Nat Med 2005;11(3):263–70.
[19] Judge AD Sood V, Shaw JR, Fang D, McClintock K, MacLachlan I. Sequence-dependent stimulation of the mammalian innate immune response by synthetic siRNA. Nat Biotechnol 2005;23(4):457–62.
[20] Sioud M. Induction of inflammatory cytokines and interferon responses by double-stranded and single-stranded siRNAs is sequence-dependent and requires endosomal localization. J Mol Biol 2005;348(5):1079–90.
[21] Yew NS, Zhao H, Wu IH, Song A, Tousignant JD, Przybylska M, et al. Reduced inflammatory response to plasmid DNA vectors by elimination and inhibition of immunostimulatory CpG motifs. Mol Ther 2000;1(3):255–62.
[22] Morrissey DV, Lockridge JA, Shaw L, Blanchard K, Jensen K, Breen W, et al. Potent and persistent in vivo anti-HBV activity of chemically modified siRNAs. Nat Biotechnol 2005;23(8):1002–7.
[23] Zimmermann TS, Lee AC, Akinc A, Bramlage B, Bumcrot D, Fedoruk MN, et al. RNAi-mediated gene silencing in non-human primates. Nature 2006;441(7089):111–4.
[24] Kim DH, Longo M, Han Y, Lundberg P, Cantin E, Rossi JJ. Interferon induction by siRNAs and ssRNAs synthesized by phage polymerase. Nat Biotechnol 2004;22(3):321–5.
[25] Tousignant JD, Gates AL, Ingram LA, Johnson CL, Nietupski JB, Cheng SH, et al. Comprehensive analysis of the acute toxicities induced by systemic administration of cationic lipid: plasmid DNA complexes in mice. Hum Gene Ther 2000;11(18): 2493–513.
[26] Kawakami S, Ito Y, Charoensit P, Yamashita F, Hashida M. Evaluation of proinflammatory cytokine production induced by linear and branched polyethylenimine/plasmid DNA complexes in mice. J Pharmacol Exp Ther 2006;317(3):1382–90.
[27] Loisel S, Le Gall C, Doucet L, Ferec C, Floch V. Contribution of plasmid DNA to hepatotoxicity after systemic administration of lipoplexes. Hum Gene Ther 2001;12(6):685–96.
[28] Sorensen DR, Leirdal M, Sioud M. Gene silencing by systemic delivery of synthetic siRNAs in adult mice. J Mol Biol 2003;327(4): 761–6.
[29] Khoury M, Louis-Plence P, Escriou V, Noel D, Largeau C, Cantos C, et al. Efficient new cationic liposome formulation for systemic delivery of small interfering RNA silencing tumor necrosis factor alpha in experimental arthritis. Arthritis Rheum 2006;54(6): 1867–77.

Available online at www.sciencedirect.com
ScienceDirect
Journal of Controlled Release 116 (2006) 330–336
journal of controlled release
www.elsevier.com/locate/jconrel

PEGylated lysine dendrimers for tumor-selective targeting after intravenous injection in tumor-bearing mice

Tatsuya Okuda [a,b], Shigeru Kawakami [a], Naomi Akimoto [a], Takuro Niidome [c], Fumiyoshi Yamashita [a], Mitsuru Hashida [a,*]

[a] *Department of Drug Delivery Research, Graduate School of Pharmaceutical Sciences, Kyoto University, 46-29 Yoshida-Shimoadachi-cho, Sakyo-ku, Kyoto 606-8501, Japan*
[b] *Japan Association for the Advancement of Medical Equipment, 3-42-6 Hongo, Bunkyo-ku, Tokyo113-0033, Japan*
[c] *Department of Applied Chemistry, Faculty of Engineering, Kyushu University, 744 Motooka, Nishi-ku, Fukuoka 819-0395, Japan*

Received 11 August 2006; accepted 25 September 2006
Available online 30 September 2006

Abstract

In this study, we synthesized a sixth generation lysine dendrimer (KG6) and two PEGylated derivatives thereof and evaluated their biodistribution characteristics in both normal and tumor-bearing mice. The intact KG6 showed a rapid clearance from the blood stream and non-specific accumulation in the liver and kidney. In contrast, the PEGylated derivatives showed a better retention in blood and low accumulativeness in organs dependent of the rate of PEGylation. In addition, PEGylated KG6 with a high modification rate was accumulated effectively in tumor tissue via the enhanced permeability and retention (EPR) effect. Moreover, we clarified that multiple administrations did not affect the biodistribution characteristics of a second dose of PEGylated KG6. PEGylated lysine dendrimer would be a useful material for a clinically applicable tumor-targeting carrier.

Keywords: Drug carrier; EPR effect; Lysine dendrimers; PEGylation; Tumor targeting

1. Introduction

Augmenting the drug concentration in tumor tissue with high selectivity is the most worthwhile subject of current cancer chemotherapy using macromolecular drug formulations. Although almost all anti-cancer drugs are pharmacologically active, the clinical application of these drugs is limited due to low solubility, unfavorable biodistribution characteristics, and serious side effects. Therefore, improving their disadvantageous biodistribution is important not only to reduce toxicity but also to boost the therapeutic effect of anti-cancer drugs. It has been reported that, the modification of a biocompatible polymer, polyethylene glycol (PEG), can extend retention time in blood by decreasing non-specific interactions with endogenous components and macrophages. For instance, Doxil® is a representative commercialized PEGylated liposomal formulation of doxorubicin [1]. In this formulation, a PEGylated liposome, i.e. STEALTH® liposome, enhances therapeutic effect and decreases serious side effects such as cardiotoxicity of doxorubicin by improving its biodistribution [2]. Furthermore, it has been reported that macromolecules having long blood retention and ~200 nm in size, such as PEGylated liposomal or polymeric formulations, effectively accumulate into the solid tumor tissue via the enhanced permeability and retention (EPR) effect. However, small and narrow sized drug carriers would be certain to be delivered to even small sized tumors by the EPR effect.

One candidate for a small and narrow sized drug carrier is a dendrimer, but little information is available on the tumor-selective disposition of (PEGylated) dendrimers after intravenous administration. Recently, dendritic polymers like polyamidoamine (PAMAM) dendrimer, which is a typical dendrimer, have attracted great attention in terms of biomedical

* Corresponding author. Fax: +81 75 753 4575.
E-mail address: hashidam@pharm.kyoto-u.ac.jp (M. Hashida).

0168-3659/$ - see front matter © 2006 Elsevier B.V. All rights reserved.
doi:10.1016/j.jconrel.2006.09.012

applications [3,4]. Although the PAMAM dendrimer has already been tested as a carrier for drugs and genes and as a contrast agent for bioimaging [5–10], it has been reported to be cytotoxic [11]. In order to construct a highly safe carrier molecule, we designed a lysine dendrimer taking into consideration the safety of the constituent unit, and employed L-lysines as branch units. We have developed a sixth generation of lysine dendrimer (KG6), which produces highly branched dendritic polymers [12]. Indeed, lysine dendrimers showed no significant cytotoxicity in cultured cells compared with PAMAM dendrimer [12]. Since lysine dendrimers have many reactive primary amino groups derived from the α- and ε-amino groups of the L-lysine residue on their surface [13], they can be modified by several functional groups. More recently, we have evaluated the disposition characteristics of lysine dendrimers and PEGylated KG6 and demonstrated that most of lysine dendrimers were accumulated in the liver, but PEGylated KG6 was sustained in the blood after intravenous administration in mice [14]. These observations prompted us to investigate whether PEGylated KG6 could be delivered to tumors selectively in tumor-bearing mice.

In this study, the physicochemical properties of PEGylated KG6 derivatives were evaluated. After the radiolabeling with [^{111}In] of PEGylated KG6 derivatives, the disposition characteristics were analyzed in tumor-bearing mice after intravenous administration. The effect of administration number of PEGylated KG6 derivatives was also evaluated for clinical use.

2. Materials and methods

2.1. Chemicals

Di-*t*-butyl dicarbonate (Boc_2O) was purchased from Peptide Institute, Inc. (Osaka, Japan). The organic solvents used for synthesis, lysine monohydrochloride, and hexamethylenediamine were obtained from Wako Pure Chemical Industries, Ltd. (Osaka, Japan). Trifluoroacetic acid, dicyclohexyl amine (DCHA), and triethylamine were purchased from Nacalai Tesque, Inc. (Kyoto, Japan). The coupling reagents, 2-(*1H*-benzotriazole-1-yl)-1,1,3,3-tetramethyluronium hexafluorophosphate (HBTU) and 1-hydroxybenzotriazol (HOBt) were acquired from Novabiochem, Merk Ltd. (Tokyo, Japan). The DTPA anhydride was purchased from Dojindo (Kumamoto, Japan). The $^{111}InCl_3$ was kindly provided by Nihon Medi-Physics Co. Ltd. (Hyogo, Japan).

2.2. Synthesis of lysine dendrimers and conjugation with DTPA

Lysine monohydrochloride was dissolved in distilled water, and a 2.2 M equivalent of Boc_2O in dioxane was added. The pH of the reaction mixture was adjusted to 8.0 or higher with 1 M NaOH. After overnight stirring at room temperature, dioxane was evaporated and the product was extracted to ethylacetate. The organic phase was washed three times with 10% citric acid and saturated NaCl, respectively, and then evaporated. *N*-Boc protected lysine was crystallized by petroleum ether with an equivalent molar ratio of DCHA. Lysine dendrimers were synthesized according to a method reported previously [12]. In brief, for the first generation synthesis, the 2.2 M excess of *N*-Boc protected lysines were coupled with hexamethylenediamine in DMF by the HBTU–HOBt method [15], and then, de-protection was achieved with TFA treatment. For the 2nd and higher generations, the coupling reaction between the amino group-free previous generation of dendrimers and *N*-Boc protected lysines was performed in DMF by the HBTU–HOBt method, and subsequently Boc-groups were removed by TFA. We synthesized lysine dendrimers up to the sixth generation by repeating these coupling and de-protection procedures. Then KG6 was conjugated with DTPA in order to radiolabel it with ^{111}In [16]. In brief, KG6 was dissolved in 20 mM borate buffer (pH 9.8) and DTPA anhydride in dimethyl sulfoxide was added at the molar ratio of 1:1. After 1 h of mixing at room temperature, the reaction mixture was purified by ultrafiltration using VIVASPIN-20 (MWCO 5,000). The purified DTPA-labeled KG6 was then lyophilized.

2.3. PEGylation of KG6

In order to prevent steric hindrance by PEG chains on the surface of the dendrimer, the DTPA-labeled KG6 was used for PEGylation. The DTPA-labeled KG6 was dissolved in borate buffer (pH 9.8) and reacted with PEG-NHS (Mw: 5,000) at 4 °C. After an overnight incubation, the reaction mixture was ultrafiltrated using VIVASPIN (MWCO 100,000). The purified PEGylated KG6 was then lyophilized. The modification rate of surface primary amino groups by PEG-NHS was evaluated by the barium–iodine method [17].

2.4. Evaluation of physicochemical properties of KG6 and its PEGylated derivatives

KG6 and its PEGylated derivatives were dissolved in PBS (pH 7.3) at a concentration of up to 5 mg/ml, and then their particle size and zeta-potential were measured with a Zetasizer Nano ZS (Malvern Instruments Ltd., United Kingdom).

2.5. Radiolabeling of dendrimers

For the biodistribution experiments, each dendrimer was radiolabeled with ^{111}In via DTPA, according to the method of Hnatowich et al. [16]. This radiolabeling method is suitable for examining the biodistribution of macromolecules from plasma to various tissues, because radioactive metabolites, if produced after cellular uptake, are retained within cells where the uptake takes place [18,19]. A DTPA-labeled dendrimer solution dissolved in a 100 mM sodium citrate buffer (pH 5.5) at a concentration of 2 mg/ml was prepared. Twenty microliters of $^{111}InCl_3$ solution was mixed with equivalent volume of 100 mM sodium citrate buffer, and the mixture was stood for a few minutes. Forty microliters of DTPA-labeled dendrimer solution was then added and mixed well. After standing for 30 min at room temperature, the mixture was purified by gel filtration chromatography using a PD-10 column and eluted with sodium citrate buffer (pH 5.5). The appropriate fractions were selected based on their radioactivity and concentrated by ultrafiltration using VIVASPIN-20.